

Gramine derivatives targeting Ca channels and Ser/Thr phosphatases: a new dual strategy for the treatment of neurodegenerative diseases

Rocío Lajarín-Cuesta, Carmen Nanclares, Juan Alberto Arranz-Tagarro, Laura González-Lafuente, Raquel L Arribas, Monique Araújo de Brito, Luis Gandia, and Cristóbal de los Ríos

J. Med. Chem., **Just Accepted Manuscript** • DOI: 10.1021/acs.jmedchem.6b00478 • Publication Date (Web): 09 Jun 2016

Downloaded from <http://pubs.acs.org> on June 15, 2016

Just Accepted

“Just Accepted” manuscripts have been peer-reviewed and accepted for publication. They are posted online prior to technical editing, formatting for publication and author proofing. The American Chemical Society provides “Just Accepted” as a free service to the research community to expedite the dissemination of scientific material as soon as possible after acceptance. “Just Accepted” manuscripts appear in full in PDF format accompanied by an HTML abstract. “Just Accepted” manuscripts have been fully peer reviewed, but should not be considered the official version of record. They are accessible to all readers and citable by the Digital Object Identifier (DOI®). “Just Accepted” is an optional service offered to authors. Therefore, the “Just Accepted” Web site may not include all articles that will be published in the journal. After a manuscript is technically edited and formatted, it will be removed from the “Just Accepted” Web site and published as an ASAP article. Note that technical editing may introduce minor changes to the manuscript text and/or graphics which could affect content, and all legal disclaimers and ethical guidelines that apply to the journal pertain. ACS cannot be held responsible for errors or consequences arising from the use of information contained in these “Just Accepted” manuscripts.

1
2
3
4
5
6
7 Gramine derivatives targeting Ca²⁺ channels and
8
9
10
11 Ser/Thr phosphatases: a new dual strategy for the
12
13
14
15
16 treatment of neurodegenerative diseases
17
18
19
20

21 *Rocío Lajarín-Cuesta,[†] Carmen Nanclares,[†] Juan-Alberto Arranz-Tagarro,[†] Laura González-*
22 *Lafuente,^{‡,¶} Raquel L. Arribas,[†] Monique Araujo de Brito,[§] Luis Gandía,[†] Cristóbal de los*
23 *Ríos*^{†,‡}*
24
25
26
27
28
29

30 [†]Instituto Teófilo Hernando and Departamento de Farmacología y Terapéutica, Facultad de
31
32 Medicina, Universidad Autónoma de Madrid, C/ Arzobispo Morcillo, 4, 28029 Madrid, Spain
33
34

35 [§]Programa de Pós Graduação em Ciências Aplicadas a Produtos Para a Saúde, Faculdade de
36
37 Farmácia, Universidade Federal Fluminense, Niterói, RJ, Brasil
38
39

40 [‡]Servicio de Farmacología Clínica, Instituto de Investigación Sanitaria, Hospital Universitario de
41
42 la Princesa, C/ Diego de León, 62, 28006 Madrid, Spain
43
44
45
46
47
48
49
50
51
52
53
54
55
56
57
58
59
60

1
2
3
4
5
6
7 ABSTRACT
8
9

10 We describe the synthesis of gramine derivatives and their pharmacological evaluation as
11 multipotent drugs for the treatment of Alzheimer's disease. An innovative multitarget approach
12 is presented, targeting both voltage-gated Ca^{2+} channels, classically studied for
13 neurodegenerative diseases, and Ser/Thr phosphatases, which have been marginally aimed, even
14 despite their key role in protein τ dephosphorylation. Twenty five compounds were synthesized
15 and mostly their neuroprotective profile exceeded that offered by the head compound gramine. In
16 general, these compounds reduced the entry of Ca^{2+} through VGCC, as measured by Fluo-4/AM
17 and patch clamp techniques, and protected in Ca^{2+} overload-induced models of neurotoxicity,
18 like glutamate or veratridine exposures. Furthermore, we hypothesize that these compounds
19 decrease τ hyperphosphorylation based on the maintenance of the Ser/Thr phosphatase activity
20 and their neuroprotection against the damage caused by okadaic acid. Hence, we propose this
21 multitarget approach as a new and promising strategy for the treatment of neurodegenerative
22 diseases.
23
24
25
26
27
28
29
30
31
32
33
34
35
36
37
38
39
40
41
42
43
44
45
46
47
48
49
50
51
52
53
54
55
56
57
58
59
60

Introduction

Over a hundred years after Alois Alzheimer reported his observations describing a new neurodegenerative disease,¹ the battery of clinically approved drugs available to treat Alzheimer's disease (AD) patients is scarce and inefficient. Nowadays, AD patients are addressed with three cholinesterases (ChE) inhibitors (galantamine, donepezil, and rivastigmine), and memantine, a *N*-methyl-D-aspartate (NMDA) glutamate receptor blocker.² The former augments the levels of the neurotransmitter acetylcholine at the cholinergic synapsis, under the rationale of the so-called "cholinergic hypothesis".³ Memantine avoids the altered Ca^{2+} uptake by neurons through the NMDA-sensitive ionic channel-coupled receptor, relying on the theory that all neurodegenerative diseases present an imbalanced Ca^{2+} homeostasis,³ so the reduction of the cytosolic Ca^{2+} concentration in neurons could slow down the progression of such diseases. Attempts to discover better drugs acting on any of these therapeutic targets have failed.⁴ Targeting the best-documented pathophysiological hallmarks of AD, that are senile plaques, mainly formed by the amyloid β peptide ($\text{A}\beta$),⁵ and neurofibrillary tangles (NFT) generated by the aggregation of the hyperphosphorylated microtubule-stabilizing τ protein,⁶ neither have supplied more successful therapies. To face amyloidogenesis, several strategies have been studied, e.g. compounds inhibiting the synthesis of $\text{A}\beta$ (α -secretase activators, both β - and γ -secretase inhibitors, among others) or its aggregation.⁷ As far as the τ -induced NFT formation, less work, but not negligible, has been carried out, mainly devoted to the preparation of kinase enzymes inhibitors, with the goal of hindering the hyperphosphorylation of τ , as the more phosphorylated τ protein is, the more susceptibility to its self-aggregation into NFT.⁸⁻⁹

1
2
3 Nevertheless, few of these approaches have supplied drugs eligible to be studied in clinical trials
4
5 for AD. Many reasons could explain the lack of promising drugs for AD, but it seems quite
6
7 likely that, as other neurodegenerative diseases, AD features a multifactorial origin, where
8
9 various physiopathological events participate in the neuronal damage that leads to AD.¹⁰ Such
10
11 hypothesis gave rise to the multi-target approach in drug discovery, which postulates that a drug,
12
13 or the association of drugs, acting on two or more different biological targets that operate in the
14
15 pathological process, could present a more beneficial effect on AD patients than a highly potent
16
17 single-targeting drug.¹¹ Hence, during the last decade, a plethora of multi-target drug-based
18
19 strategies have been described, by combining pharmacological interventions over ChE enzymes,
20
21 A β peptides or the τ -induced NFT formation, among other therapeutic targets.¹²⁻¹⁵ In this regard,
22
23 our research group has reported several families of multi-target drugs since 2000, with the
24
25 control of neuronal Ca²⁺ homeostasis as the common target.¹⁶⁻¹⁹ Many evidences support the idea
26
27 that pharmacological modulation of Ca²⁺ homeostasis within neurons could mitigate the
28
29 neurotoxicity present in a neurodegeneration scenario,²⁰ as that neurons having NFT present high
30
31 activity of Ca²⁺-dependent protease enzymes,²¹ or that the presence of A β peptides elevates Ca²⁺
32
33 concentrations in resting neurons, sensitizing them for apoptosis phenomena.²²⁻²³ There is
34
35 preclinical and clinical evidence that the blockade of voltage-gated Ca²⁺ channels (VGCC) may
36
37 attenuate dementia, since an excessive and prolonged Ca²⁺ entry into the cytosol leads to
38
39 neurodegeneration and neuronal loss.²⁴⁻²⁶ The VGCC blockade, both at presynaptic (P/Q- and N-
40
41 type VGCC) and at postsynaptic sites (L-type VGCC), has shown a neuroprotective effect in
42
43 different animal models of neurodegeneration and excitotoxicity, such as the blockade of ω -
44
45 agatoxin IVA in a rat ischemia model (P/Q-VGCC blocker),²⁷ the blockade by the synthetic
46
47 version of ω -conotoxin MVIIA in a traumatic diffuse brain injury model in rats (N-type VGCC
48
49
50
51
52
53
54
55
56
57
58
59
60

1
2
3 blocker),²⁸ that of verapamil in a focal ischemia model in rats (L-type VGCC blocker),²⁹ or those
4
5 of nivaldipine and nitrendipine (L-type VGCC blockers) in an A β -induced toxicity model in
6
7 mice.³⁰ Some VGCC antagonists have been tested in clinical trials for dementia and, according to
8
9 the Cochrane report published in 2002, nimodipine can be of some efficacy for the treatment of
10
11 AD.³¹
12
13

14
15
16 On the other hand, during the latest years, we have paid attention to the neurodegeneration
17
18 elicited by the hyperphosphorylated τ protein and the subsequent intracellular NFT.³² The degree
19
20 of τ phosphorylation depends on the enzymatic activity of both kinases and phosphatases.⁹
21
22 Tremendous scientific efforts have been invested in the development of kinase enzymes
23
24 inhibitors, e.g. GSK3 β inhibitors,³³⁻³⁴ with scarce success. However, rather few contributions
25
26 have aimed to promote the dephosphorylation process carried out by phosphatase enzymes,³⁵
27
28 mainly performed by the phosphoprotein phosphatases (PPP) 2A and 1 (PP2A and PP1,
29
30 respectively).³⁶ PPP enzymes catalyze the hydrolysis of phosphate esters at Ser and Thr residues,
31
32 being PP1 and PP2A responsible of the 90% of the cellular Ser/Thr phosphatase activity within
33
34 healthy human brains.³⁶ In AD brains, total phosphatase activity is reduced by half, with PP2A,
35
36 PP1, and PP5 activities decreased by 50%, 20%, and 20%, respectively.³⁶⁻³⁷ Regarding to PP2A,
37
38 it is the most efficient τ phosphatase (accounts for over 70% of τ dephosphorylation).³⁵ The
39
40 relationship between the AD-triggered neurodegeneration and the downregulation of PP2A
41
42 activity has been widely demonstrated: in postmortem brains from AD patients, PP2A mRNA
43
44 and protein levels are decreased,³⁸⁻³⁹ and the endogenous PP2A inhibitors I₁^{PP2A} (nuclear) and
45
46 I₂^{PP2A} (cytoplasmatic) are increased by 20%,⁴⁰⁻⁴¹ it exists an augmented inactivation of the PP2A
47
48 catalytic subunit (PP2Ac) through the phosphorylation at Y307 residue;⁴² the PP2A methylation
49
50 rates at L309, responsible for the PP2A assembly to its regulatory subunits, is decreased;⁴³ there
51
52
53
54
55
56
57
58
59
60

1
2
3 is also a reduced expression of B55 α , the main PP2A regulatory subunit mediating
4
5
6 dephosphorylation of τ , in frontal and temporal cortex.⁴⁴⁻⁴⁶ Moreover, PP2A dephosphorylates
7
8 NMDA receptors at several NRx subunits, evoking a lesser Ca²⁺ influx through these receptors,
9
10 what entails a neuroprotective effect against excitotoxicity, similarly to that of memantine.⁴⁷⁻⁴⁸
11
12 Although the leading role of PP2A is indisputable, other PPP enzymes, like PP1 and PP5, are
13
14 also implicated in the pathology of AD.⁴⁹
15
16
17
18

19 Our research group described the neuroprotective properties of a multi-target drug that was able
20
21 to inhibit cholinesterase enzymes and to maintain the PP2A-controlled phosphatase activity.⁵⁰
22
23 Confirming the correlation between NMDA and PP2A, ethyl 5-amino-2-methyl-6,7,8,9-
24
25 tetrahydrobenzo[*b*][1,8]naphthyridine-3-carboxylate (ITH12246), protected rat hippocampal
26
27 slices against the damage elicited by glutamate through a mechanism implicating PPP, as
28
29 okadaic acid (OA), a selective inhibitor of PP1 and PP2A, reversed its neuroprotective signal. In
30
31 addition, it reduced the loss of memory in mice subjected to scopolamine administration, as
32
33 monitored by the object placement test.⁵¹
34
35
36
37
38

39 For all of these reasons, we considered worthwhile to keep deepening in the study of PPP
40
41 enzymes as a part of a multi-target strategy to find new drugs for AD, remaining the control of
42
43 cytosolic Ca²⁺ as the other main therapeutic target. In this work, we describe the findings
44
45 observed with a family of indole derivatives, analogues to the natural alkaloid gramine (**1**, Figure
46
47
48 **1**), which has shown promising pharmacological activities.⁵²
49
50
51
52
53
54
55
56
57
58
59
60

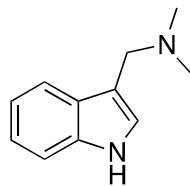
**1**

Figure 1. Chemical structure of the alkaloid gramine (3-(dimethylaminomethyl)-1*H*-indole) (**1**).

Indeed, some of its brominated derivatives have been described as Ca^{2+} channels blockers.⁵³ In our laboratory, we observed that **1** protected SH-SY5Y neuroblastoma cells against the toxic stimulus generated by OA in a wide range of concentrations. We wondered whether such huge neuroprotective effect was, at least in part, due to the activation of PPP enzymes. This prompted us to design a new family of **1** derivatives and evaluate their pharmacological activity as Ca^{2+} channel blockers and Ser/Thr phosphatase activators, as well as assessing their neuroprotective profile in several in vitro models of neurodegeneration. The results reported in this paper support the idea that scientific community devoted to the search of multi-target drugs must continue its efforts to offer original proposals for the discovery of new drugs for neurodegenerative diseases.

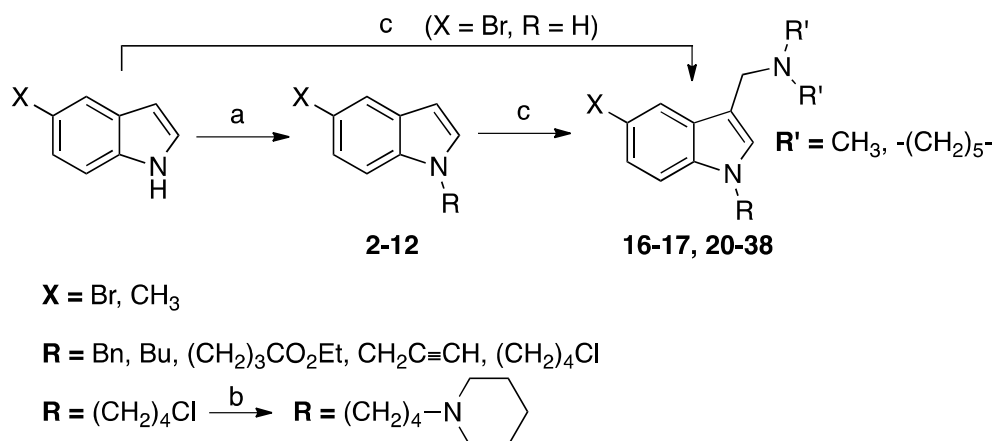
Results and Discussion

Chemistry. The design of **1** derivatives focused on favoring a potential Ca^{2+} channel blocking activity as well as the interaction with the principal dephosphorylating enzymes of τ , that are the Ser/Thr phosphatases. As two marine-derived bromo-substituted **1** analogs have been described to block VGCC,⁵³ we reasoned that our first family of synthesized **1** derivatives should possess a

1
2
3 bromine atom at C5. Regarding to the binding to PP2A, previous studies of our research group
4 detected a binding site close to the catalytic core in the PP2Ac subunit,⁵⁰ where specific ligands
5 would not compromise the PP2A enzymatic activity, but alternatively would avoid the arrival of
6 direct inhibitors to the catalytic machinery of PP2A. By preliminary computational studies, if
7 new indole-based ligands present a tiny hydrophobic substituent at C5, as well as a long
8 hydrophobic moiety linked to the indole nitrogen, their affinity to this binding site would
9 improve. Thus, a second family of **1** derivatives having a methyl group at C5 was designed,
10 where the members of both families are differentially substituted at the indole nitrogen. The *N*-
11 alkylation was carried out by nucleophilic substitution of alkyl halides in presence of NaH as a
12 base (Scheme 1). Alkyl, benzyl or propargyl bromides and iodides suffered the nucleophilic
13 attack of 5-substituted indoles in excellent yields, except for ethyl bromobutyrate, as only 5-
14 bromoindole was able to lead to the formation of the ethyl indolylbutanoate **6** in low yields.
15 Attempts to optimize this substitution, by using other bases such as KOH and solvents (DMF,
16 CH₃CN, THF or acetone), phase-transfer catalysts, among other experimental conditions, were
17 not satisfactory. The nucleophilic substitution over 1-chloro-4-iodobutane, leading to the *N*-(4'-
18 chlorobutyl)-indoles **9** and **10**, allowed us to incorporate piperidine as a pending substituent,
19 through a further nucleophilic attack of piperidine in acetonitrile, using K₂CO₃ as a base,
20 obtaining the 5-bromo or 5-methyl-*N*-substituted derivatives **11** and **12**, respectively (Scheme 1).
21 Polycations, such as polylysine and protamine, as well as highly basic compounds, specifically
22 histones, were the first compounds found to activate PP2A in vitro.⁵⁴ This fact, together with
23 other recently discovered positively charged modulators, e.g. memantine, led to establish basic
24 cationic compounds as a family of PP2A activators.⁵⁵⁻⁵⁶ The head compound **1** possesses a basic
25 amino group that is positively charged at physiological pH, so it could be classified as a cationic
26
27
28
29
30
31
32
33
34
35
36
37
38
39
40
41
42
43
44
45
46
47
48
49
50
51
52
53
54
55
56
57
58
59
60

activator. In order to keep this property, all **1** derivatives conserve this basic amino group at C3, either as dimethylamine or piperidine group.

Scheme 1. Preparation of **1** derivatives^a

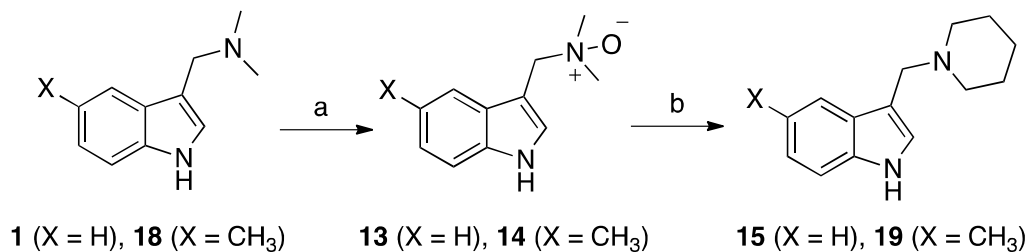


^aReagents and Conditions: (a) (1) NaH, DMSO, rt, 1–2 h; (2) alkyl halide, rt, 1–12 h. (b) piperidine, MeCN, K₂CO₃, rt to 60 °C, 12 h. (c) Me₂NH or piperidine, HCHO (aq), AcOH, 0 °C to rt, 2 to 5 h.

The further Mannich type reaction furnished the desired C3-substituted **1** derivatives **20–38** in which the order of addition of reagents played an essential role, allowing us to reach excellent yields. 5-Bromoindole reacted with dimethylamine or piperidine at these conditions to form the *N*-unsubstituted **1** derivatives **16** and **17** in good yields (Scheme 1). However, the same protocol proposed for the reaction of 5-methylindole with piperidine, derived in a complex mixture of products. To sort this out, we selected an alternative method conducted through the generation of the *N*-oxide intermediate **14**, from the commercially available 5-methylgramine **18**, which is

further treated with neat piperidine to form compound **19** in quantitative yield. The same strategy was proposed to prepare the piperidine-bearing analogue of **1**, that is compound **15**, synthesized and pharmacologically evaluated for comparative purposes (Scheme 2).

Scheme 2. Alternative route for the preparation of *N*-unsubstituted **1 derivatives^a**



^aReagents and conditions: (a) H₂O₂ (30% aq), EtOH, rt, 2 h. (b) piperidine, reflux, 3 h.

At this point, it is worthwhile mentioning that, despite the huge literature in both Organic and Medicinal Chemistry regarding to the syntheses and uses of 3-aminoethylindoles, backed by the Chemistry of the tryptophan, serotonin and melatonin, among other so-called biogenic amines,⁵⁷⁻⁵⁹ the study of the 3-aminomethylindoles analogs has been comparatively inappreciable. Indeed, **1** derivatives have been extensively used in Organic Synthesis as starting material for the preparation of serotonin-like natural products and potential drugs.⁶⁰⁻⁶¹ Among the reasons for this lack of interest, their delicate chemical stability in aqueous acid media seems to be the main reason.⁶² We confirmed by ¹H-NMR that 3-methylen-3*H*-indoles are formed as by-products after routine procedures such as silica gel-based flash chromatography purification or in the NMR analysis when using CDCl₃ as deuterated solvent. These pitfalls were avoided by executing the work-up at pH 14, neutralizing the organic solvents, mainly CH₂Cl₂, with basic alumina and, when necessary, purification with flash chromatography was carried out in basic alumina instead

1
2
3 of silica gel, and NMR spectra were made in acetone-*d*₆. After confirming the structure and
4
5 purity of final compounds **15–38**, with the aim of facilitating their manipulation and biological
6
7 evaluation, they were salinized to hydrochloride or oxalate salts, by treatment with HCl in ether
8
9 or oxalic acid in ethyl acetate solutions, respectively. Solvents for the salinization solutions were
10
11 previously dried over MgSO₄ to remove possible traces of water. We then confirmed structure
12
13 and purity of the salinized compounds, and their chemical stability at physiological pH by
14
15 monitoring ¹³C and ¹H-NMR spectra in D₂O, not detecting any modification in the NMR signals
16
17 after several days.
18
19
20
21

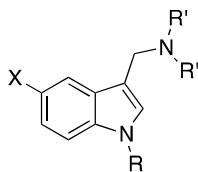
22 **Pharmacological Evaluation. Effect of 1 derivatives 15–38 on the Ca²⁺ entry through**

23 **VGCC.** To evaluate the blocking activity of the new **1** derivatives, we stimulated SH-SY5Y
24
25 neuroblastoma cells with an extracellular solution containing KCl 70 mM, leading to membrane
26
27 depolarization and VGCC opening.⁶³ The SH-SY5Y neuroblastoma cell line is a reliable model
28
29 to monitor cytosolic Ca²⁺ fluctuations in excitable cells, as it possesses VGCC and intracellular
30
31 Ca²⁺-buffering organelles similarly to regular primary neuronal cultures.⁶⁴⁻⁶⁵ Consequently, the
32
33 SH-SY5Y cells, charged with the Ca²⁺-sensitive fluorescent probe Fluo-4, suffered a rise in the
34
35 cytosolic Ca²⁺ that was modulated by the presence of these potential VGCC blockers, tested at 1
36
37 μM (Table 1). Eleven out 24 compounds reduced the high K⁺-evoked cytosolic Ca²⁺ increase in a
38
39 statistically significant manner. Considering the data expressed in Table 1, some structure-
40
41 activity relationships can be inferred. Most of the compounds that block VGCC bear a
42
43 piperidinylmethyl substituent at C3; compound **20** (X = Br, R = Bn) was the only
44
45 dimethylaminomethyl-substituted compound, together with **1**, that reduced the Ca²⁺ increase. As
46
47 far as the *N*-alkylation, the benzyl moiety affords the best blockade of Ca²⁺ increase, but also
48
49 butyl, chlorobutyl, and propargyl groups are optimal substituents, whose results are fairly better
50
51
52
53
54
55
56
57
58
59
60

1
2
3 when compounds present additionally a bromine atom at C5 and a piperidine at C3, instead of
4 methyl and dimethylamine, respectively. It is already known in literature that bromo-substitution
5 at the indole core provides compounds with Ca^{2+} antagonist activity.⁵³ The blocking effect of
6 compounds that present a bulky substituent at the indole nitrogen (**27**, **28**, **35–38**) substantially
7 dropped to below 20%. The well-known VGCC blocker nifedipine,⁶⁶ used as a standard at 3 μM ,
8 reduced Ca^{2+} increase by 73% in these experiments. With the goal of deepening into their Ca^{2+} -
9 antagonist effect, we carried out electrophysiological techniques, performing patch-clamp
10 experiments in the whole-cell configuration. We studied the effect on Ca^{2+} (I_{Ca}) currents of **1**, the
11 best VGCC blockers of the family (**21**, **25**, **30**, and **33**), and three more compounds (**20**, **23**, and
12 **26**) that showed important neuroprotective and/or pro-phosphatases properties (see below).

13
14
15
16
17
18
19
20
21
22
23
24
25
26
27 Current vs. voltage (I/V) curves, from -60 to $+60$ mV as depolarizing potentials, were initially
28 performed in absence of compounds, to select the depolarizing pulse that featured the highest
29 I_{Ca} . Then, bovine chromaffin cells were subjected to 50 ms depolarizing pulses every 20 s at the
30 potential at which maximal I_{Ca} was obtained, usually 0 mV; after reaching a stable response,
31 cells were perfused with the different compounds until a maximal blockade degree was achieved.
32
33
34
35
36
37
38
39
40
41
42
43
44
45
46
47
48
49
50
51
52
53
54
55
56
57
58
59
60
Figure S1 of supporting info reflects a typical register of I_{Ca} , dealing with a control situation.
Under these experimental conditions, compounds **1**, **21**, **23**, **25**, and **26** blocked I_{Ca} in a
statistically significant manner (Figure 2), confirming their VGCC blocking properties.

Table 1. Blockade by compounds 15–38 of the Ca^{2+} entry elicited by K^+ 70 mM-evoked depolarization in SH-SY5Y cells, measured by the Ca^{2+} -sensitive probe Fluo-4/AM^a



Comp.	X	R	R'	% Blockade
Nifedipine ^b	-	-	-	73 ± 5 ^{***}
1	H	H	CH ₃	25 ± 7 ^{**}
15	H	H	-(CH ₂) ₅ -	30 ± 4 ^{**}
16	Br	H	CH ₃	3 ± 3 ^{ns}
17	Br	H	-(CH ₂) ₅ -	7 ± 7 ^{ns}
18	CH ₃	H	CH ₃	10 ± 5 ^{ns}
19	CH ₃	H	-(CH ₂) ₅ -	16 ± 6 ^{ns}
20	Br	Bn	CH ₃	38 ± 6 ^{***}
21	Br	Bn	-(CH ₂) ₅ -	45 ± 3 ^{***}
22	CH ₃	Bn	CH ₃	18 ± 6 ^{ns}
23	CH ₃	Bn	-(CH ₂) ₅ -	22 ± 9 [*]
24	Br	<i>n</i> -Bu	CH ₃	14 ± 6 ^{ns}
25	Br	<i>n</i> -Bu	-(CH ₂) ₅ -	63 ± 4 ^{***}
26	CH ₃	<i>n</i> -Bu	-(CH ₂) ₅ -	21 ± 6 [*]
27	Br	-(CH ₂) ₃ CO ₂ Et	CH ₃	13 ± 6 ^{ns}
28	Br	-(CH ₂) ₃ CO ₂ Et	-(CH ₂) ₅ -	16 ± 3 ^{ns}
29	Br	CH ₂ C≡CH	CH ₃	10 ± 5 ^{ns}
30	Br	CH ₂ C≡CH	-(CH ₂) ₅ -	42 ± 3 ^{***}
31	CH ₃	CH ₂ C≡CH	CH ₃	14 ± 6 ^{ns}
32	CH ₃	CH ₂ C≡CH	-(CH ₂) ₅ -	25 ± 7 ^{**}
33	Br	-(CH ₂) ₄ Cl	-(CH ₂) ₅ -	57 ± 6 ^{***}
34	CH ₃	-(CH ₂) ₄ Cl	-(CH ₂) ₅ -	35 ± 5 ^{***}
35	Br	-(CH ₂) ₄ Pi	CH ₃	14 ± 6 ^{ns}
36	Br	-(CH ₂) ₄ Pi	-(CH ₂) ₅ -	19 ± 7 [*]
37	CH ₃	-(CH ₂) ₄ Pi	CH ₃	16 ± 7 ^{ns}
38	CH ₃	-(CH ₂) ₄ Pi	-(CH ₂) ₅ -	4 ± 3 ^{ns}

^aData are mean of at least six experiments ± SEM comparing with the K⁺-induced Ca²⁺ increase in absence of compounds. Compounds assayed at 1 μM. ^{***} *p* < 0.001, ^{**} *p* < 0.01, ^{*} *p* < 0.05, and ns = not significant. ^b Tested at 3 μM. Pi = piperidinyl.

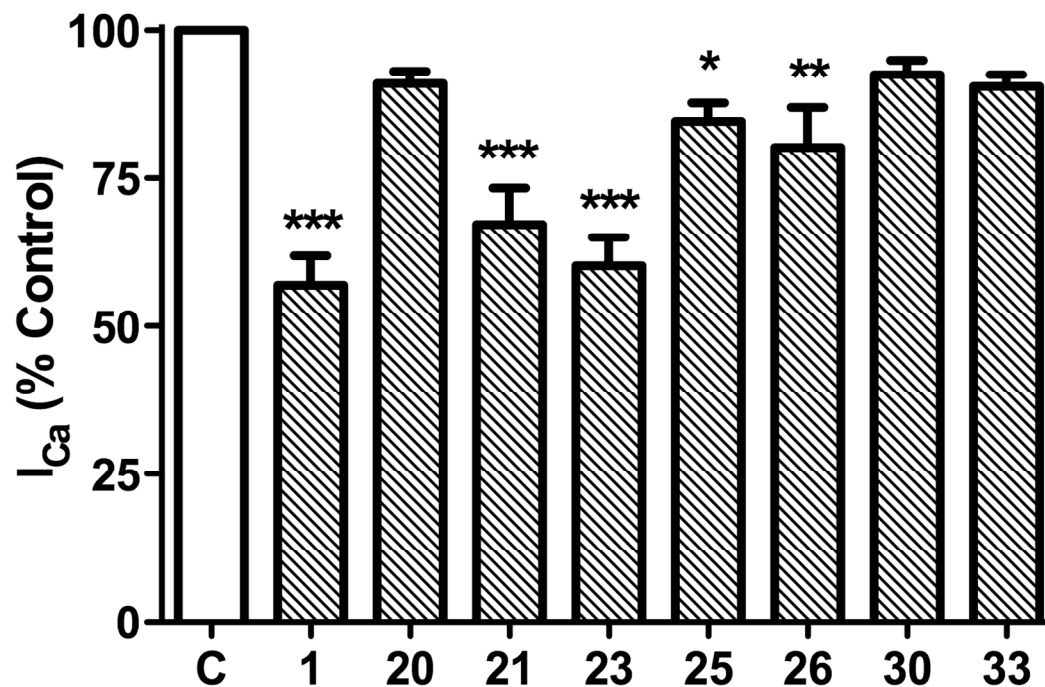
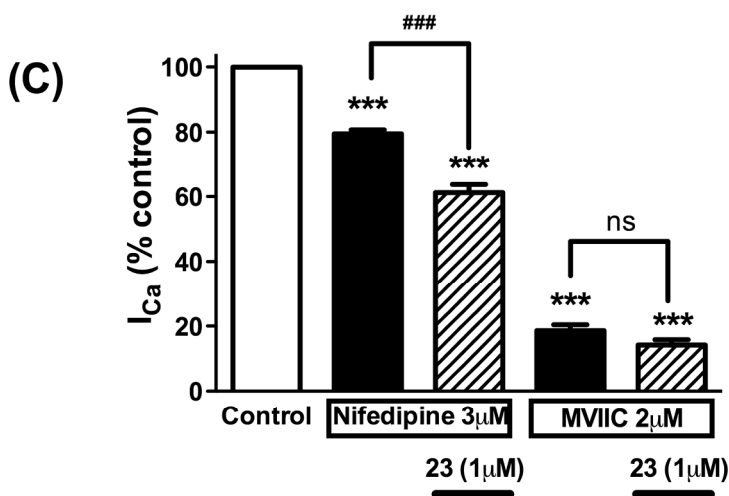
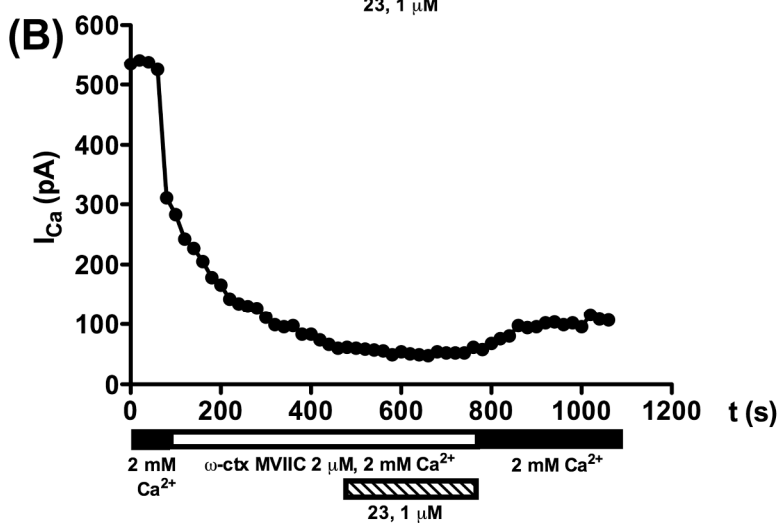
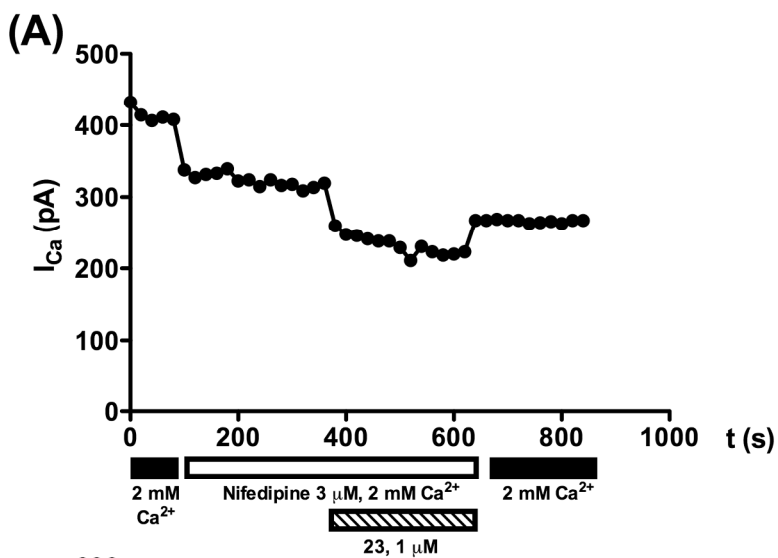


Figure 2. Depolarization-evoked Ca^{2+} currents (I_{Ca}) in bovine chromaffin cells. Whole-cell I_{Ca} were recorded using 2 mM Ca^{2+} as charge carrier and -80 mV as holding potential. Averaged results, of at least 7 cells of independent batches, representing normalized remaining I_{Ca} in presence of selected **1** derivatives at the concentration of 1 μ M. *** $p < 0.001$, ** $p < 0.01$, * $p < 0.05$, comparing with control in absence of compounds (C, white bar).

Of note is the differential behavior of these compounds between the two experimental procedures realized, i.e. the fluorescent-based assay and the patch-clamp techniques. This could be interpreted in base of the different expression of VGCC subtypes between SH-SY5Y cells, where 50% of them belong to the L-subtype,⁶⁴ and bovine chromaffin cells, which only present a 20% of the L-subtype.⁶⁷ Such hypothesis raised an important point, as compound **23** blocked I_{Ca} in bovine chromaffin cells by 40% (Figure 2), but it only reduced the fluorescence-monitored Ca^{2+} increase in SH-SY5Y by 22% (Table 1), so we wondered whether compound **23** could be

1
2
3 selectively blocking the non L-subtypes of VGCC, what it would be of interest taking into
4
5 account the lack of efficient pharmacological tools available to selectively interact to such non-L
6
7 VGCC,⁶⁸ either N- or P/Q subtypes. For this reason, we further registered the VGCC blocking
8
9 effect of compound **23** in presence of the selective L-type VGCC blocker nifedipine, as well as
10
11 in presence of the N and P/Q type VGCC blocker ω -conotoxin MVIIC,⁶⁹ as shown in Figure 3.
12
13 Compound **23** exerted an additional blockade of the I_{Ca} in the presence of nifedipine (Figure 3A
14
15 and 3C), but on the contrary, the I_{Ca} observed in the presence of ω -conotoxin MVIIC remained
16
17 constant when compound **23** was administered (Figure 3B and 3C). Therefore, we can conclude
18
19 that compound **23** is acting as a selective non-L VGCC blocker.
20
21
22
23
24
25
26
27
28
29
30
31
32
33
34
35
36
37
38
39
40
41
42
43
44
45
46
47
48
49
50
51
52
53
54
55
56
57
58
59
60



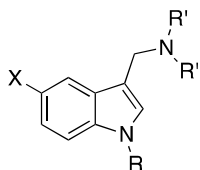
1
2
3 **Figure 3.** Compound **23** partially blocks non-L type Ca^{2+} currents. Bovine chromaffin cells,
4 voltage-clamped at -80 mV, were challenged with 50 ms depolarizing pulses to 0 mV at 20 s
5 intervals. Ca^{2+} 2 mM was used as charge carrier. Panel A shows typical Ca^{2+} currents (I_{Ca}) time
6 course in a cell perfused with nifedipine 3 μM (L-type VGCC blocker) alone and in the presence
7 of compound **23** at 1 μM . Panel B shows a typical I_{Ca} time course in a cell perfused with ω -
8 conotoxin (ω -ctx) MVIIC 2 μM (N- and P/Q-type Ca^{2+} VGCC blocker) alone and in the
9 presence of compound **23** at 1 μM . Panel C shows the averaged peak amplitude of I_{Ca} with
10 respect to control (white bar) in the presence of either nifedipine or MVIIC alone (black
11 columns) or concomitantly with compound **23** (stripped columns). Data are means \pm SEM of 16
12 cells for each treatment from 3 different cell cultures. $^{***}p < 0.001$, respect to cells depolarized in
13 absence of drugs (control group), $^{###}p < 0.001$, ns = not significant.
14
15
16
17
18
19
20
21
22
23
24
25
26
27
28
29
30
31
32

33 **Effect of 1 derivatives 15–38 on the Ser/Thr phosphatase activity.** As mentioned in the
34 introduction, the Ser/Thr phosphatase activity of PP1 and PP2A is impaired in neurodegeneration
35 scenarios,³⁶ leading to the augmentation of the phosphorylation rate in τ protein, and thus
36 favoring its self-aggregation to form the NFT. This reduction in the phosphatase activity is
37 mainly ascribed to the concurrence of endogenous inhibitors that bind at the catalytic site of PPP,
38 hindering the hydrolysis of phosphate esters at Ser or Thr amino acids.⁴⁰ The use of the PP1 and
39 PP2 inhibitor OA is a reliable model of these pathological processes, as it has been described that
40 it tightly binds catalytic subunits of both enzymes.⁷⁰ Indeed, the administration of OA to rodents
41 mimicked the morphological hallmarks of AD.⁷¹ Hence, to appraise the effect of compounds **15–**
42 **38** on the activity of PPP enzymes, we subjected SH-SY5Y cells to the exposure of OA at 15
43 nM, an adequate concentration to inhibit both PP1 and PP2A,⁷²⁻⁷³ in the presence of the testing
44
45
46
47
48
49
50
51
52
53
54
55
56
57
58
59
60

1
2
3 compounds, estimating the resulting phosphatase activity by the colorimetric method of the *p*-
4 nitrophenylphosphate (pNPP). The pNPP is a colorless substance that turns yellow (absorbance
5 405 nm) when is hydrolyzed to *p*-nitrophenol by the action of phosphatase enzymes.⁷⁴ Under
6 these experimental conditions, OA diminished the total phosphatase activity by a 32%, and 12
7 out of 25 compounds reduced the deprival of total phosphatase activity in a statistically
8 significant manner, being the best compounds able to maintain such enzymatic activity a 40%
9 higher than with OA in absence of compounds (Table 2). Although OA interacts exclusively
10 with the Ser/Thr phosphatases PP1 and PP2A, due to the Tyr phosphatase activity is much more
11 extended in nervous system than the Ser/Thr phosphatase activity, we decided to study the effect
12 of the compounds in presence of the Tyr phosphatase inhibitor sodium orthovanadate,⁷⁵
13 administered to the SH-SY5Y cells at 1 mM, so the phosphatase activity recorded by the pNPP
14 probe would be only derived from Ser/Thr phosphatase enzymes. Pretty much similar data were
15 found; half of the compounds counteracted the OA-induced reduction of the Ser/Thr phosphatase
16 activity in a statistically significant manner (Table 2). Regarding to structure-activity
17 relationships, either no substitution at the indole nitrogen (R = H), benzyl group or a butyl group,
18 seem to be the most optimal alternatives as R substituents, as hit compound **1** offers a
19 satisfactory pro-phosphatase activity, similarly to compounds **15**, **16**, **18**, **20**, **23**, **24**, **25**, and **31**.

20
21
22 Collectively, compounds **15**, **23**, and **25**, together with the hit compound **1**, featured a multitarget
23 activity, as they demonstrated both pro-phosphatase and Ca²⁺ channels blocking activities, in all
24 the experimental protocols implemented. In parallel, we evaluated the capability of the **1**
25 derivatives **15–38** to protect against neuronal damage in in vitro models of neurodegeneration
26 resembling AD.
27
28
29
30
31
32
33
34
35
36
37
38
39
40
41
42
43
44
45
46
47
48
49
50
51
52
53
54
55
56
57
58
59
60

Table 2. Effect of 1 derivatives 15–38 on the Ser/Thr phosphatase activity depressed by okadaic acid (OA)^a



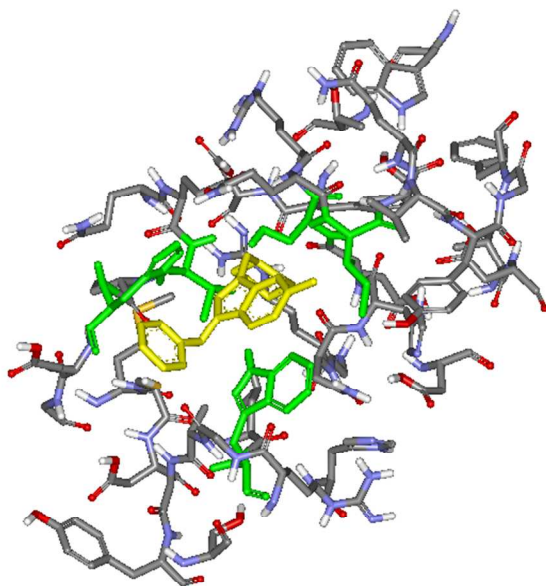
Comp.	X	R	R'	% Total phosphatase activity	% Ser/Thr phosphatase activity
Control	-	-	-	100	100
OA	-	-	-	68 ± 2 ^{###}	61 ± 3 ^{###}
Memantine	-	-	-	77 ± 3 [*]	78 ± 5 ^{***}
1	H	H	CH ₃	80 ± 5 [*]	76 ± 5 [*]
15	H	H	-(CH ₂) ₅ -	76 ± 4 [*]	79 ± 8 [*]
16	Br	H	CH ₃	80 ± 4 ^{**}	76 ± 6 [*]
17	Br	H	-(CH ₂) ₅ -	74 ± 4 ^{ns}	67 ± 3 ^{ns}
18	CH ₃	H	CH ₃	79 ± 4 [*]	77 ± 4 [*]
19	CH ₃	H	-(CH ₂) ₅ -	71 ± 3 ^{ns}	69 ± 5 ^{ns}
20	Br	Bn	CH ₃	81 ± 4 ^{**}	78 ± 5 [*]
21	Br	Bn	-(CH ₂) ₅ -	79 ± 4 [*]	70 ± 7 ^{ns}
22	CH ₃	Bn	CH ₃	73 ± 3 ^{ns}	66 ± 5 ^{ns}
23	CH ₃	Bn	-(CH ₂) ₅ -	77 ± 4 [*]	78 ± 6 [*]
24	Br	<i>n</i> -Bu	CH ₃	81 ± 6 [*]	76 ± 4 [*]
25	Br	<i>n</i> -Bu	-(CH ₂) ₅ -	78 ± 3 [*]	79 ± 4 ^{**}
26	CH ₃	<i>n</i> -Bu	-(CH ₂) ₅ -	69 ± 2 ^{ns}	66 ± 6 ^{ns}
27	Br	(CH ₂) ₃ CO ₂ Et	CH ₃	76 ± 7 ^{ns}	66 ± 4 ^{ns}
28	Br	(CH ₂) ₃ CO ₂ Et	-(CH ₂) ₅ -	73 ± 2 ^{ns}	71 ± 3 [*]
29	Br	CH ₂ C≡CH	CH ₃	70 ± 5 ^{ns}	64 ± 4 ^{ns}
30	Br	CH ₂ C≡CH	-(CH ₂) ₅ -	77 ± 3 ^{**}	72 ± 5 ^{ns}
31	CH ₃	CH ₂ C≡CH	CH ₃	80 ± 4 [*]	74 ± 9 [*]
32	CH ₃	CH ₂ C≡CH	-(CH ₂) ₅ -	71 ± 3 ^{ns}	66 ± 7 ^{ns}
33	Br	-(CH ₂) ₄ Cl	-(CH ₂) ₅ -	68 ± 3 ^{ns}	62 ± 7 ^{ns}
34	CH ₃	-(CH ₂) ₄ Cl	-(CH ₂) ₅ -	71 ± 4 ^{ns}	62 ± 6 ^{ns}
35	Br	-(CH ₂) ₄ Pi	CH ₃	73 ± 5 ^{ns}	68 ± 5 ^{ns}

36	Br	-(CH ₂) ₄ Pi	-(CH ₂) ₅ -	73 ± 2 [*]	70 ± 4 ^{ns}
37	CH ₃	-(CH ₂) ₄ Pi	CH ₃	74 ± 3 ^{ns}	68 ± 5 ^{ns}
38	CH ₃	-(CH ₂) ₄ Pi	-(CH ₂) ₅ -	72 ± 3 ^{ns}	70 ± 5 [*]

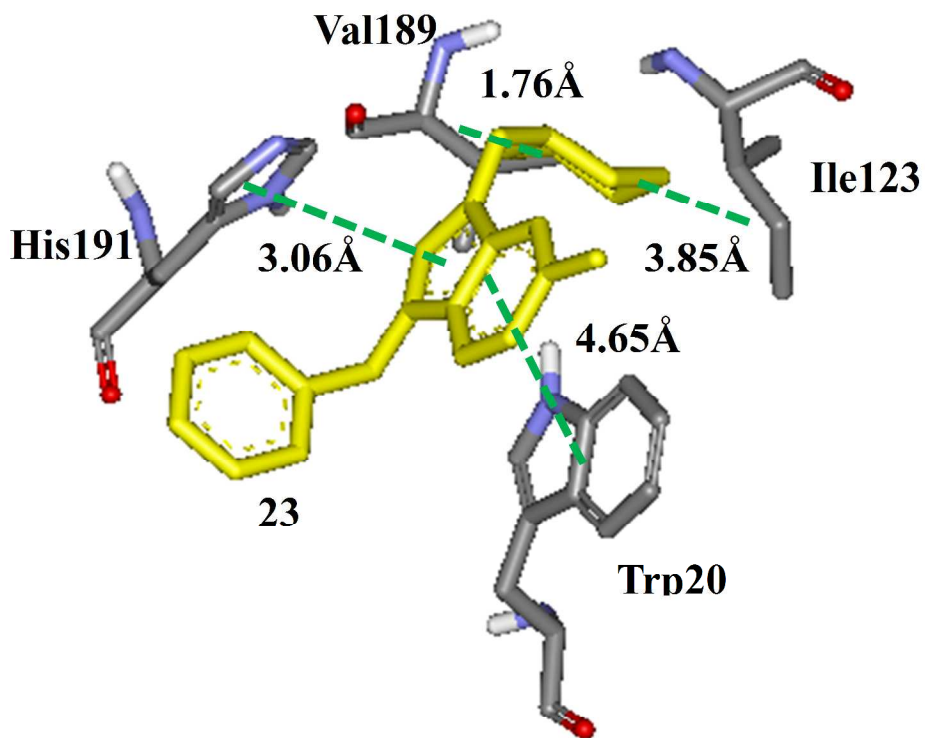
^aSH-SY5Y cells were treated with compounds at 0.1 μM in presence of the PPP inhibitor okadaic acid (OA) at 15 nM. Data are mean of at least four experiments ± SEM, expressed as percentage respect to control situation, where cells were not treated with compounds neither OA. ^{###}*p* < 0.001, respect to control; ^{***}*p* < 0.001, ^{**}*p* < 0.01, ^{*}*p* < 0.05, and ns = not significant, respect to cells only treated with OA. Phosphatase activity was evaluated by the method of the pNPP. To estimate Ser/Thr phosphatase activity, the Tyr phosphatase inhibitor sodium orthovanadate at 1 mM was applied to the experiments. Pi = piperidinyl.

Docking studies. We selected compound **23** to exemplify the interaction between the main τ protein phosphatase, i.e. PP2A, with these **1** derivatives, because of its significant phosphatase activity (Table 2), as well as its neuroprotective activity counteracting the damage provoked by OA and Glu (Table 3 and Figure 5, see below). The complex of PP2A and compound **23** revealed van der Waals interactions between the piperidine ring of compound **23** and the side chain of residues Ile123 (d = 3.85 Å) and Val189 (d = 1.76 Å) (Figure 4B). The indole ring of compound **23** also interacts with both the imidazole ring of His191 (d = 3.06 Å) and the indole ring of the Trp200 (d = 4.65 Å), probably in a hydrophobic π- π stacking contact (Figure 4B). OA also interacted with Ile123, His191 and Trp200, as previously reported by Xing *et al.*, 2006.⁷⁰ Also, the nitrogen of the piperidine ring of compound **23** probably makes a strong hydrogen bond with the hydroxyl group of Ser120 (d = 1.66 Å) (Figure 4C), which contributes to the affinity of the ligand in this binding site of PP2A (Figure 4A).

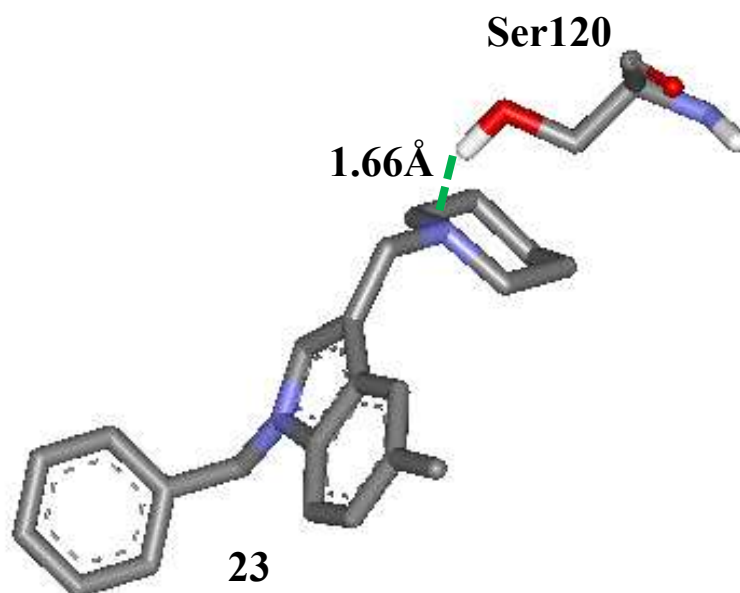
(A)



(B)



1
2
3
4 (C)
5
6
7
8
9
10
11
12
13
14
15
16
17
18
19
20
21
22
23
24
25
26
27
28
29



30 **Figure 4.** Docking of the compound **23**–PP2A complex. (A) Pose of compound **23** (yellow) in
31 the PP2Ac binding site (main residues in green). (B) Van der Waals contacts (Val189 and
32 Ile123) and hydrophobic π interactions (His191 and Trp200) of compound **23** (yellow). (C)
33 Hydrogen bond between compound **23** and Ser120 (Energy scores provided in Table S1 of
34 supporting information).
35
36
37
38
39
40
41
42
43
44
45

46 **Neuroprotection experiments.** Since we had found some bioactive compounds, the raised
47 question was whether these **1** derivatives, by regulating the neuronal Ca^{2+} homeostasis and the
48 Ser/Thr phosphatase activity, would be able to protect neurons against neurotoxic stimuli related
49 to AD. We monitored cell viability with the method of the 3-(4,5-dimethylthiazol-2-yl)-2,5-
50 diphenyltetrazolium bromide (MTT) reduction,⁷⁶ in in vitro neuronal models subjected to Ca^{2+}
51
52
53
54
55
56
57
58
59
60

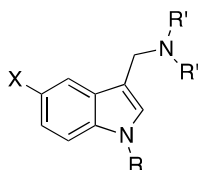
1
2
3 overload or τ hyperpolarization. Since VGCC and Ser/Thr phosphatases, targeted by our **1**
4 derivatives, present highlighted physiological roles, we firstly assessed the potential per se
5 toxicity of compounds **15–38** in the neuronal models object of study, i.e. cortical motor neurons
6 and SH-SY5Y neuroblastoma cells. As graphed in Figures S2 and S3 of supporting info, none of
7 the compounds, incubated for 48 h, reduced the cell viability of SH-SY5Y cells at concentrations
8 lower than 10 μM . In the case of cortical motor neurons, compounds **15** and **36** marginally
9 reduced cell viability when incubated for 48 h at 1 μM (Figures S4 and S5, supporting info).

10
11
12
13
14
15
16
17
18
19
20
21 In order to emulate a Ca^{2+} overload, cortical motor neurons were exposed to veratridine 20 μM , a
22 voltage-gated Na^+ channels (VGNC) ligand that delays their inactivation, leading to a
23 depolarization-elicited Ca^{2+} entry.⁷⁷ After 24 h pre-incubation of the compounds, at 1 μM ,
24 neurons were co-incubated for another 24 h with veratridine (20 μM), inducing a loss of viability
25 of about 50% (Table 3). More than a half of the compounds, but not **1**, reduced the veratridine-
26 induced damage in a significant manner. Compounds **23**, **25**, and **26** stood out by rescuing the
27 neuronal viability by a 50% or more. In these experiments, the presence of piperidine at C3
28 instead of dimethylamine seems to favor this neuroprotective activity. Again, benzyl and butyl
29 groups branched to the indole nitrogen afforded the best neuroprotection (Table 3). The VGNC
30 blocker tetrodotoxin (TTX) was used as standard in these experiments.⁷⁸

31
32
33
34
35
36
37
38
39
40
41
42
43
44
45
46
47 In parallel, we tested the neuroprotective activity of compounds **15–38** against a model of τ
48 hyperphosphorylation, by stimulating SH-SY5Y neuroblastoma cells with the PPP selective
49 inhibitor OA. SH-SY5Y cells suffered a fall of 35% in their viability when exposed for 20 h to
50 OA 20 nM. Under this situation, most of compounds noticeably mitigated the reduction in the
51 cell viability caused by OA, and 10 of them did it by 50% or more, being the best compound **25**
52
53
54
55
56
57
58
59
60

(Table 3). Melatonin was used as standard in these experiments.⁷⁹ Among all the structure-activity relationships considered, we appreciated outstanding activities when the compounds present benzyl, butyl or no substitution at the indole nitrogen.

Table 3. %Neuroprotection of 1 derivatives 15–38 on the cell viability of cortical motor neurons and SH-SY5Y neuroblastoma cells damaged with veratridine and okadaic acid, respectively^a



Comp.	X	R	R'	Veratridine ^b	Okadaic acid ^c
TTX	-	-	-	77 ± 1 ^{***}	-
Melatonin	-	-	-	-	43 ± 3 ^{***}
1	H	H	CH ₃	0 ± 4 ^{ns}	45 ± 2 ^{***}
15	H	H	-(CH ₂) ₅ -	18 ± 7 ^{ns}	47 ± 5 ^{**}
16	Br	H	CH ₃	11 ± 5 ^{ns}	47 ± 4 ^{**}
17	Br	H	-(CH ₂) ₅ -	19 ± 3 [*]	60 ± 5 ^{**}
18	CH ₃	H	CH ₃	30 ± 5 [*]	59 ± 4 ^{**}
19	CH ₃	H	-(CH ₂) ₅ -	7 ± 3 ^{ns}	38 ± 3 ^{***}
20	Br	Bn	CH ₃	34 ± 3 ^{***}	56 ± 3 ^{***}
21	Br	Bn	-(CH ₂) ₅ -	36 ± 6 ^{**}	54 ± 6 ^{**}
22	CH ₃	Bn	CH ₃	35 ± 9 [*]	44 ± 4 [*]
23	CH ₃	Bn	-(CH ₂) ₅ -	51 ± 6 ^{**}	56 ± 5 ^{**}
24	Br	<i>n</i> -Bu	CH ₃	34 ± 5 ^{**}	66 ± 5 ^{**}
25	Br	<i>n</i> -Bu	-(CH ₂) ₅ -	72 ± 7 ^{***}	71 ± 3 ^{***}
26	CH ₃	<i>n</i> -Bu	-(CH ₂) ₅ -	60 ± 7 ^{***}	46 ± 5 [*]
27	Br	(CH ₂) ₃ CO ₂ Et	CH ₃	42 ± 6 [*]	58 ± 2 ^{**}
28	Br	(CH ₂) ₃ CO ₂ Et	-(CH ₂) ₅ -	36 ± 7 [*]	43 ± 5 [*]
29	Br	CH ₂ C≡CH	CH ₃	17 ± 5 ^{ns}	12 ± 4 ^{ns}

30	Br	CH ₂ C≡CH	-(CH ₂) ₅ -	24 ± 4 [*]	47 ± 3 ^{**}
31	CH ₃	CH ₂ C≡CH	CH ₃	14 ± 10 ^{ns}	12 ± 3 ^{ns}
32	CH ₃	CH ₂ C≡CH	-(CH ₂) ₅ -	19 ± 5 ^{ns}	42 ± 8 ^{ns}
33	Br	-(CH ₂) ₄ Cl	-(CH ₂) ₅ -	39 ± 6 [*]	48 ± 8 [*]
34	CH ₃	-(CH ₂) ₄ Cl	-(CH ₂) ₅ -	36 ± 5 ^{**}	56 ± 6 [*]
35	Br	-(CH ₂) ₄ Pi	CH ₃	21 ± 9 ^{ns}	31 ± 3 ^{**}
36	Br	-(CH ₂) ₄ Pi	-(CH ₂) ₅ -	0 ± 5 ^{ns}	61 ± 4 ^{***}
37	CH ₃	-(CH ₂) ₄ Pi	CH ₃	4 ± 6 ^{ns}	37 ± 1 ^{***}
38	CH ₃	-(CH ₂) ₄ Pi	-(CH ₂) ₅ -	1 ± 5 ^{ns}	26 ± 3 ^{**}

^aCell viability was measured by the method of the MTT reduction. Data are expressed as the percentage of cell viability recovered in cells treated with the toxic stimulus plus compounds, comparing with viability of cells only exposed to veratridine or OA; mean of at least 5 experiments ± SEM in triplicate. ^{***}*p* < 0.001, ^{**}*p* < 0.01, ^{*}*p* < 0.05, and ns = not significant, respect to cells only treated with veratridine or OA. ^bCortical motor neurons exposed to veratridine 20 μM in presence of compounds at 1 μM, except for compound **36** which was tested at 0.1 μM due to its toxicity at 1 μM (see Figure S5 supporting info). ^cSH-SY5Y neuroblastoma cells exposed to OA 20 nM in presence of compounds at 0.1 μM. Pi = piperidinyl.

Gathering all the pharmacological data obtained, we proposed that these new **1** derivatives are multitarget neuroprotective compounds able to interact with two pathophysiological events involved in AD, i.e. Ca²⁺ dishomeostasis and Ser/Thr phosphatases inhibition, and in turn entailing a neuroprotective profile, according to the in vitro models of neurodegeneration we have performed. Overall, it can be extrapolated that the presence of benzyl or butyl groups at the indole nitrogen along with a piperidine at C3, preferentially offer privileged structures of **1** derivatives, according to the pharmacological activities object of study, and their consequent neuroprotective properties over AD-resembling neurodegeneration models. However,

1
2
3 neuroprotective compounds historically fail in their pharmacological actions when they are
4
5 evaluated in more physiological models of experimental study. Therefore, we carry out a more
6
7 physiological model of biological evaluation, defined by the use of rat hippocampal slices
8
9 subjected to toxic stimuli related to AD, recording the ability of selected compounds to
10
11 counteract the tissue damage.^{17, 50, 63, 80} In this preparation, neurons are surrounded by their natural
12
13 environment, e.g. glia cells, extracellular matrix, etc. Rat hippocampi were subjected to a
14
15 sustained exposition to the excitatory neurotransmitter glutamate, which is considered a close
16
17 model to the excitotoxicity occurred in neurodegeneration.⁸¹ In addition, recent contributions
18
19 have hypothesized that PP2A can down-regulate the Ca²⁺ influx through the NMDA receptors, as
20
21 dephosphorylation of NR1A subunit by this phosphatase accelerates the desensitization rate of
22
23 the NMDA receptor.^{48, 82-83} Hence, this model has proven to be an excellent experimental protocol
24
25 to test the neuroprotective activities of either Ca²⁺-antagonists or Ser/Thr phosphatase activators.
26
27 Tested compounds were selected according to optimal biological activities and neuroprotective
28
29 properties in vitro, as well as chemical diversity (Figure 5).
30
31
32
33
34
35
36
37
38
39
40
41
42
43
44
45
46
47
48
49
50
51
52
53
54
55
56
57
58
59
60

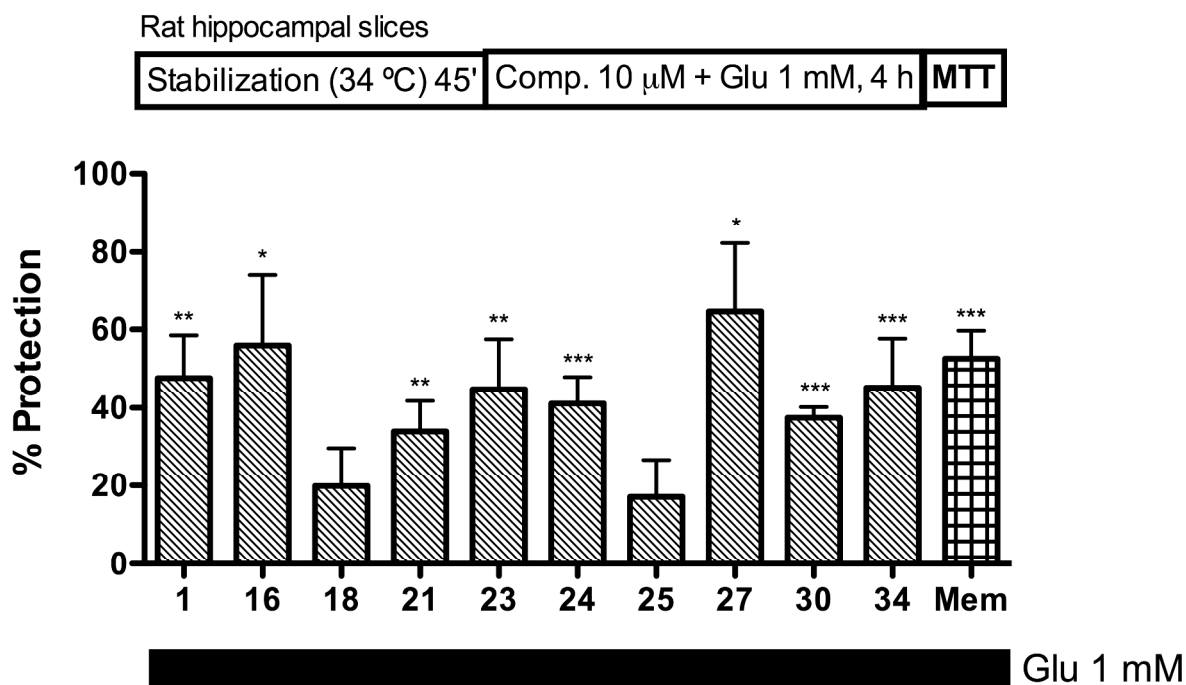


Figure 5. Effect of selected **1** derivatives on the viability of rat hippocampal slices damaged with glutamate (Glu) 1 mM, measured through the MTT reduction. %Protection respect to the viability of hippocampal slices treated with Glu in absence of compounds. Data are expressed as mean \pm SEM of at least 4 different tissue batches in quadruplicate. *** $p < 0.001$, ** $p < 0.01$, * $p < 0.05$, respect to slices only treated with Glu.

Compounds **21**, **23**, and **30** that had evinced regulating activities of both Ca^{2+} entry and Ser/Thr phosphatases, and protected neurons in both veratridine and OA-based models of neurodegeneration, avoided the glutamate-induced loss of viability of the hippocampal slices by 30% or more, however the multitarget and in vitro neuroprotectant compound **25** failed to protect such preparations. Compounds **16**, **18**, and **24**, behaved as Ser/Thr phosphatase activators (Table 2), and had a proper in vitro neuroprotection profile. Nevertheless, in this model, only

1
2
3 compounds **16** and **24** reasserted that neuroprotective properties, as they reduced the damage by
4 glutamate by 40% or more (Figure 5). Compound **34** also protected hippocampi from the
5 glutamate excitotoxicity, according to its in vitro neuroprotection properties (Table 3), although
6
7
8 glutamate excitotoxicity, according to its in vitro neuroprotection properties (Table 3), although
9
10 it had only targeted the cell Ca^{2+} signal (Table 1). Compound **27** protected against both Ca^{2+}
11
12 overload and τ hyperphosphorylation, but it did not show any activity on either depolarization-
13
14 evoked Ca^{2+} entry or Ser/Thr phosphatase. In addition, it substantially protected hippocampal
15
16 slices against the glutamate exposure (Figure 5); one possibility is that compound **27** would be
17
18 affecting other pathways involved in the neuronal death/survival scenarios.
19
20
21
22
23
24
25
26

27 **Conclusions**

28
29
30 This work illustrates an alternative approach for a multitarget strategy for the treatment of AD,
31
32 by devising a double interaction with neuronal Ca^{2+} signaling and Ser/Thr phosphatase activity.
33
34 Regulation of cytosolic Ca^{2+} concentrations by different VGCC blockers has been a
35
36 pharmacology target widely studied for several neurodegenerative diseases, but few
37
38 contributions has selected it as a part of a multitarget-based drug development, which have
39
40 mostly inclined towards the complement of cholinesterases inhibition with $\text{A}\beta$ down-regulation
41
42 or τ hyperphosphorylation reduction strategies, affording unfruitful results. Regarding to the τ
43
44 hyperphosphorylation, the research works have almost exclusively focused on the development
45
46 of protein τ kinase inhibitors. We propose that the activation, or the reduction of inhibitory
47
48 actions, over protein τ phosphatase enzymes, deserves more attention, overcoming the historical
49
50 prejudice of their unspecificity, currently rebutted.³² Of note is that, when we recorded the
51
52 phosphatase activity by the method of the pNPP (Table 2), a substantial decrease of 70% was
53
54
55
56
57
58
59
60

1
2
3 computed in cells exposed to the Tyr phosphatase inhibitor VO_3^- , what confirms that Tyr
4
5 phosphatase activity is much more extended than Ser/Thr phosphatase activity in nervous
6
7 system. The fact that τ protein is mainly dephosphorylated by PP1 and PP2A entails the
8
9 advantage that Ser/Thr phosphatase activators would not present such sizeable off-target
10
11 pharmacology as Tyr phosphatase activators would. To finish up, we hypothesize that compound
12
13 **23** is an eligible lead compound to further investigate its pharmacological activities in preclinical
14
15 models of AD, as it demonstrated significant activity over VCGG and Ser/Thr phosphatases,
16
17 accompanied by a wide-spectrum neuroprotective profile. The fact that compound **23** exerts Ca^{2+}
18
19 blockade preferentially through non-L type VGCC is in agreement to the rising interest of
20
21 developing both N- and P/Q type VGCC blockers for dementia,^{68, 84} what supposes a
22
23 breakthrough in the study of Ca^{2+} antagonists for central nervous system diseases because they
24
25 could bypass the cardiovascular side effects resulting from peripheral L-type channel blockade,²⁵⁻
26
27 ²⁶ Hence, the derivative 1-benzyl-5-methyl-3-(piperidin-1-ylmethyl)-1*H*-indole (compound **23**,
28
29 which we have named ITH12657) features an innovative multitarget-based mechanism of action,
30
31 aiming neuronal Ca^{2+} control and Ser/Thr phosphatase activity.
32
33
34
35
36
37
38
39
40
41
42

43 **Experimental Section**

44
45
46 **General Procedures.** 5-Bromoindole, 5-methylindole, **1**, compound **18**, and general reagents
47
48 were purchased from Sigma-Aldrich (Madrid, Spain). Solvents were purchased from VWR
49
50 (Barcelona, Spain). Reactions were monitored by thin layer chromatography aluminum oxide on
51
52 TLC-PET foils (Sigma-Aldrich). Detection was made with UV light at 254 nm. All the reactions
53
54 were subjected to Schlenk conditions (vacuum purges and argon atmosphere). Pre-charged basic
55
56
57
58
59
60

1
2
3 aluminum oxide (Brockmann I) columns were used in a Biotage chromatographic station.
4
5 Melting points were determined in a Stuart apparatus (SMP-10) and are not corrected. MS
6
7 spectra were obtained in a QSTAR de ABSciex apparatus. ^1H and ^{13}C NMR spectra were carried
8
9 out with a Bruker AVANCE 300 MHz and described as ppm using deuterated solvents as
10
11 internal standard. All the compounds described and pharmacologically tested had a purity of
12
13 95% or more determined by elemental analysis performed on a LECO CHNS-932 station (C, H,
14
15 and N within 0.4% of the calculated values for the proposed formula). None of the tested
16
17 compounds present structural similarities with Pan Assay Interference Compounds (PAINS),
18
19 according to the classification reported by Baell and Holloway.⁸⁵
20
21
22
23
24

25
26 **General Method for the Synthesis of *N*-alkyl-5-bromo(or methyl)indoles 2–10.** The method
27
28 described by Na et al.⁸⁶ was followed, with slight modifications. Briefly, to a solution of 5-
29
30 bromo-1*H*-indole or 5-methyl-1*H*-indole (1 equiv) in anhydrous dimethyl sulfoxide (DMSO)
31
32 (1.4–5 mL/mmol), NaH (1.2 equiv, 60%, dispersed in mineral oil) was added under inert gas at
33
34 room temperature. After the reaction mixture was stirred for 1–2 h, the corresponding alkyl
35
36 halide (1.2–1.7 equiv) was added and stirred for 1–2 h more (with exception of the synthesis of
37
38 **6**, which required overnight), monitored by TLC. When the reaction was completed, it was
39
40 stopped by addition of water (10 mL/mmol) and extracted with neutralized CH_2Cl_2 (3×30
41
42 mL/mmol). The organic layer was dried over anhydrous Na_2SO_4 , filtered and evaporated, to
43
44 obtain a yellow oil that did not require purification, except for compound **6**.
45
46
47
48
49

50
51 **1-Benzyl-5-bromo-1*H*-indole (2).** Following the general method for the synthesis of *N*-alkyl-5-
52
53 bromo(or methyl)indoles **2–10**, reaction of 5-bromo-1*H*-indole (500 mg, 2.55 mmol) in
54
55 anhydrous DMSO (13 mL) with NaH (122 mg, 3.06 mmol) and benzyl bromide (363 μL , 3.06
56
57 mmol) yielded **2** (740 mg, >99%) with spectral data according to literature.⁸⁷
58
59
60

1
2
3 **1-Benzyl-5-methyl-1*H*-indole (3)**. Following the general method for the synthesis of *N*-alkyl-5-
4 bromo(or methyl)indoles **2–10**, reaction of 5-methyl-1*H*-indole (150 mg, 1.14 mmol) in
5
6 anhydrous DMSO (5.71 mL) with NaH (55 mg, 1.37 mmol) and benzyl bromide (163 μ L, 1.37
7
8 mmol) yielded **3** (282 mg, >99%) with spectral data according to literature.⁸⁸
9
10

11
12
13 **5-Bromo-1-butyl-1*H*-indole (4)**. Following the general method for the synthesis of *N*-alkyl-5-
14 bromo(or methyl)indoles **2–10**, reaction of 5-bromo-1*H*-indole (200 mg, 1.02 mmol) in
15
16 anhydrous DMSO (5 mL) with NaH (48 mg, 1.22 mmol) and 1-iodobutane (139 μ L, 1.22 mmol)
17
18 yielded **4** (242 mg, 94%). ¹H NMR (300 MHz, CDCl₃) δ 7.75 (d, 1H, *J* = 1.8 Hz, H4), 7.27 (dd,
19
20 1H, *J* = 1.9, 8.7 Hz, H6), 7.19 (d, 1H, *J* = 8.7 Hz, H7), 7.09 (d, 1H, *J* = 3.1 Hz, H2), 6.42 (d, 1H,
21
22 *J* = 3.1 Hz, H3), 4.09 (t, 2H, *J* = 7.1 Hz, NCH₂), 1.81 (m, 2H, NCH₂CH₂), 1.36–1.24 (m, 2H,
23
24 CH₂CH₃), 0.94 (t, 3H, *J* = 7.3 Hz, CH₃).
25
26
27
28
29
30

31
32 **1-Butyl-5-methyl-1*H*-indole (5)**. Following the general method for the synthesis of *N*-alkyl-5-
33 bromo(or methyl)indoles **2–10**, reaction of 5-methyl-1*H*-indole (200 mg, 1.52 mmol) in
34
35 anhydrous DMSO (7.62 mL) with NaH (73 mg, 1.83 mmol) and 1-iodobutane (208 μ L, 1.83
36
37 mmol) yielded **5** (235 mg, 82%). ¹H NMR (300 MHz, acetone-*d*₆): δ 7.38 (m, 1H, H4), 7.29 (d,
38
39 1H, *J* = 8.4 Hz, H7), 7.16 (d, 1H, *J* = 3.1 Hz, H2), 7.01 (dd, 1H, *J* = 1.6, 8.4 Hz, H6), 6.37 (dd,
40
41 1H, *J* = 0.8, 3.1 Hz, H3) 4.11 (t, 2H, = 7.0 Hz, NCH₂), 2.44 (s, 3H, CH₃), 1.78 (m, 2H,
42
43 NCH₂CH₂), 1.35–1.24 (m, 2H, CH₂CH₃), 0.93 (t, 3H, *J* = 7.4 Hz, CH₂CH₃).
44
45
46
47
48

49
50 **Ethyl 4-(5-bromo-1*H*-indol-1-yl)butanoate (6)**. Following the general method for the synthesis
51 of *N*-alkyl-5-bromo(or methyl)indoles **2–10**, reaction of 5-bromo-1*H*-indole (500 mg, 2.55
52
53 mmol) in anhydrous DMSO (10 mL) with NaH (122 mg, 3.06 mmol) and ethyl 4-
54
55 bromobutanoate (461 μ L, 3.06 mmol) obtaining a yellow solid that was purified by automatized
56
57
58
59
60

1
2
3
4
5
6
7
8
9
10
11
12
13
14
15
16
17
18
19
20
21
22
23
24
25
26
27
28
29
30
31
32
33
34
35
36
37
38
39
40
41
42
43
44
45
46
47
48
49
50
51
52
53
54
55
56
57
58
59
60

flash chromatography with ethyl acetate/hexane mixtures as eluent, yielding **6** (281 mg, 36%).

^1H NMR (300 MHz, acetone- d_6) δ 7.76 (d, 1H, J = 1.8 Hz, H4), 7.42 (d, 1H, J = 8.7 Hz, H7), 7.31–7.26 (m, 2H, H2, H6), 6.47 (dd, 1H, J = 0.6, 3.1 Hz, H3), 4.24 (t, 2H, J = 7.0 Hz, NCH₂), 4.09 (c, 2H, J = 7.1 Hz, OCH₂), 2.28 (t, 2H, J = 6.8 Hz, CH₂CO), 2.10 (m, 2H, NCH₂CH₂), 1.20 (t, 3H, J = 7.1 Hz, CH₃).

5-Bromo-1-(prop-2-yn-1-yl)-1H-indole (7). Following the general method for the synthesis of *N*-alkyl-5-bromo(or methyl)indoles **2–10**, reaction of 5-bromo-1*H*-indole (200 mg, 1.02 mmol) in anhydrous DMSO (2.5 mL) with NaH (48 mg, 1.22 mmol) and 3-bromoprop-1-yne (136 μL , 1.22 mmol) yielded **7** (235 mg, >99%), with spectral data according to literature.⁸⁹

5-Methyl-1-(prop-2-yn-1-yl)-1H-indole (8). Following the general method for the synthesis of *N*-alkyl-5-bromo(or methyl)indoles **2–10**, reaction of 5-methyl-1*H*-indole (150 mg, 1.14 mmol) in anhydrous DMSO (2.29 mL) with NaH (55 mg, 1.37 mmol) and 3-bromoprop-1-yne (153 μL , 1.372 mmol) yielded **8** (190 mg, >99%). ^1H NMR (300 MHz, acetone- d_6) δ 7.51 (m, 1H, H4), 7.41 (d, 1H, J = 8.3 Hz, H7), 7.28 (d, 1H, J = 3.2 Hz, H2), 7.16 (dd, 1H, J = 1.5, 8.4 Hz, H6), 6.54 (dd, 1H, J = 0.8, 3.2 Hz, H3), 4.88 (d, 2H, J = 2.6 Hz, CH₂), 2.91 (t, 1H, J = 2.6 Hz, CH), 2.39 (s, 3H, CH₃).

5-Bromo-1-(4-chlorobutyl)-1H-indole (9). Following the general method for the synthesis of *N*-alkyl-5-bromo(or methyl)indoles **2–10**, reaction of 5-bromo-1*H*-indole (1 g, 5.10 mmol) in anhydrous DMSO (7 mL) with NaH (245 mg, 6.12 mmol) and 1-chloro-4-iodobutane (1.1 mL, 8.67 mmol) yielded **9** (1.4 g, >99%). ^1H NMR (300 MHz, CDCl₃) δ 7.77 (d, 1H, J = 1.8 Hz, H4), 7.30 (dd, 1H, J = 1.9, 8.7 Hz, H6), 7.20 (d, 1H, J = 8.7 Hz, H7), 7.09 (d, 1H, J = 3.1 Hz, H2),

1
2
3 6.45 (dd, 1H, $J = 0.6, 3.1$ Hz, H3), 4.13 (t, 2H, $J = 6.9$ Hz, NCH₂), 3.50 (t, 2H, $J = 6.4$ Hz,
4 CH₂Cl), 2.05–1.93 and 1.80–1.68 (2m, 4H, ClCH₂CH₂CH₂).

5
6
7
8
9 **1-(4-Chlorobutyl)-5-methyl-1H-indole (10)**. Following the general method for the synthesis of
10 *N*-alkyl-5-bromo(or methyl)indoles **2–10**, reaction of 5-methyl-1*H*-indole (200 mg, 1.52 mmol)
11 in anhydrous DMSO (6 mL) with NaH (73 mg, 1.83 mmol) and 1-chloro-4-iodobutane (317 μL,
12 2.59 mmol) yielded **10** (340 mg, >99%). ¹H NMR (300 MHz, acetone-*d*₆) δ 7.38 (m, 1H, H4),
13 7.31 (d, 1H, $J = 8.4$ Hz, H7), 7.18 (d, 1H, $J = 3.1$ Hz, H2), 7.01 (dd, 1H, $J = 1.3$ Hz, $J = 8.4$ Hz,
14 H6), 6.38 (dd, 1H, $J = 0.7, 3.1$ Hz, H3), 4.15 (t, 2H, $J = 6.9$ Hz, NCH₂), 3.53 (t, 2H, $J = 6.6$ Hz,
15 CH₂Cl), 2.43 (s, 3H, CH₃), 1.98–1.87 and 1.76–1.65 (2m, 4H, ClCH₂CH₂CH₂).

16
17
18
19
20
21
22
23
24
25
26
27 **General Method for the synthesis of 4-(piperidin-1-yl)butylindoles 11 and 12**. The method
28 of Martelli et al.⁹⁰ was followed with slight modifications. To a solution of 1-(4-
29 chlorobutyl)indole **9** or **10** (1 equiv) and piperidine (1.2 equiv) in CH₃CN (6.9 mL/mmol),
30 anhydrous K₂CO₃ (1–2 equiv) was added at room temperature. The reaction mixture was stirred
31 at 60 °C overnight, under inert gas. When the reaction did not further evolve, monitored by TLC,
32 it was cooled down and neutralized CH₂Cl₂ (10 mL/mmol) was added. The mixture was then
33 basified with NaOH 10%_{aq} (30 mL/mmol), extracted with neutralized CH₂Cl₂ (2 × 30
34 mL/mmol), dried over anhydrous Na₂SO₄, filtered, and evaporated under vacuum. The crude was
35 purified by automatized flash chromatography in basic alumina with ethyl acetate/hexane
36 mixtures as eluent, obtaining a colorless oil.
37
38
39
40
41
42
43
44
45
46
47
48
49
50

51 **5-Bromo-1-(4-(piperidin-1-yl)butyl)-1H-indole (11)**. Following the general method for the
52 synthesis of 4-(piperidin-1-yl)butylindoles **11** and **12**, reaction of **9** (107 mg, 0.37 mmol) with
53 piperidine (44 μL, 0.45 mmol) and anhydrous K₂CO₃ (52 mg, 0.37 mmol) yielded **11** (70 mg,
54
55
56
57
58
59
60

1
2
3
4
5
6
7
8
9
10
11
12
13
60%). ^1H NMR (300 MHz, acetone- d_6) δ 7.72 (d, 1H, J = 1.8 Hz, H4), 7.44 (d, 1H, J = 8.7 Hz, H7), 7.33 (d, 1H, J = 3.1 Hz, H2), 7.24 (dd, 1H, J = 1.9, 8.7 Hz, H6), 6.43 (dd, 1H, J = 0.7, 3.2 Hz, H3), 4.22 [t, 2H, J = 7.1 Hz, $\text{NCH}_2(\text{CH}_2)_3\text{N}$], 2.33–2.19 [m, 6H, $\text{N}(\text{CH}_2)_3\text{CH}_2\text{N}$, H2'], 1.85 [m, 2H, $\text{NCH}_2\text{CH}_2(\text{CH}_2)_2\text{N}$], 1.54–1.29 [m, 8H, $\text{N}(\text{CH}_2)_2\text{CH}_2\text{CH}_2\text{N}$, H3', H4'].

14
15
16
17
18
19
20
21
22
23
24
25
26
27
28
29
30
31
32
33
5-Methyl-1-(4-(piperidin-1-yl)butyl)-1H-indole (12). Following the general method for the synthesis of 4-(piperidin-1-yl)butylindoles **11** and **12**, reaction of **10** (328 mg, 1.48 mmol) with piperidine (176 μL , 1.78 mmol) and anhydrous K_2CO_3 (409 mg, 2.96 mmol), yielded **12** (180 mg, 45%). ^1H NMR (300 MHz, acetone- d_6) δ 7.36 (m, 1H, H4), 7.32 (d, 1H, J = 8.4 Hz, H7), 7.17 (d, 1H, J = 3.1 Hz, H2), 6.98 (dd, 1H, J = 1.2, 8.1 Hz, H6), 6.35 (dd, 1H, J = 0.7, 3.1 Hz, H3), 4.13 [t, 2H, J = 7.1 Hz, $\text{NCH}_2(\text{CH}_2)_3\text{N}$], 2.42 (s, 3H, CH_3), 2.32–2.19 [m, 6H, $\text{N}(\text{CH}_2)_3\text{CH}_2\text{N}$, H2'], 1.83 [m, 2H, $\text{NCH}_2\text{CH}_2(\text{CH}_2)_2\text{N}$], 1.57–1.28 [m, 8H, $\text{N}(\text{CH}_2)_2\text{CH}_2\text{CH}_2\text{N}$, H3', H4'].

34
35
36
37
38
39
40
41
42
43
44
45
46
47
48
49
50
51
52
53
54
55
56
57
58
59
60
General Method for the synthesis of 15 and 19 through N-oxide intermediates. Based on the method of Henry and Leete,⁹¹ with modifications. To a suspension of **1** or *N,N*-dimethyl-1-(5-methyl-1*H*-indol-3-yl)methanamine (1 equiv) in absolute ethanol (0.4 mL/mmol), H_2O_2 (30 %; 0.3 mL/mmol) was added, under inert gas at room temperature, observing a slight exothermicity and the complete dissolution of the suspension. Then, the magnet stir was removed and the flask cooled down with an ice bath and thus kept overnight. The white crystals formed were washed with absolute ethanol and the supernatant was discarded. After confirming the formation of the corresponding *N*-oxide by ^1H NMR, they were dissolved in piperidine (4 mL/mmol) and refluxed for 3 hours. Piperidine was evaporated under vacuum and the crude recrystallized in absolute ethanol to obtain pure compounds.

1
2
3 **3-(Piperidin-1-ylmethyl)-1*H*-indole (15)**. Following the general method for the synthesis of **15**
4 and **19** through *N*-oxide intermediates, reaction of **1** (200 mg, 1.15 mmol) with H₂O₂ (30 %; 0.3
5 mL) in absolute ethanol (0.46 mL), yielded the 1-(1*H*-indol-3-yl)-*N,N*-dimethylmethanamine
6 mL) in absolute ethanol (0.46 mL), yielded the 1-(1*H*-indol-3-yl)-*N,N*-dimethylmethanamine
7 oxide **13**⁹¹ that was immediately used with no further purification. ¹H NMR (300 MHz, CD₃OD)
8 δ 7.70 (ddd, 1H, *J* = 0.8, 1.4, 7.7 Hz, H4), 7.56 (s, 1H, H2), 7.42 (ddd, 1H, *J* = 0.8, 1.2, 8.0 Hz,
9 H7), 7.21–7.10 (m, 2H, H5, H6), 4.61 (s, 2H, CH₂), 3.11 [s, 6H, (CH₃)₂]. Reaction of **13** (230
10 mg, 1.21 mmol) in piperidine (4.6 mL) yielded **15** (191 mg, 74%) as a brown crystal. Mp 142–
11 144 °C. ¹H NMR (300 MHz, CD₃OD) δ 7.64 (d, 1H, *J* = 7.8 Hz, H4), 7.39 (m, 1H, H7), 7.24 (s,
12 1H, H2), 7.16–7.02 (m, 2H, H5, H6), 3.76 (s, 2H, CH₂), 2.56 (m, 4H, H2'), 1.63 (m, 4H, H3'),
13 1.52–1.41 (m, 2H, H4'). ¹³C NMR (75.4 MHz, CD₃OD) δ 137.8, 129.6, 126.3, 122.3, 120.0,
14 119.6, 112.2, 110.7, 55.0, 54.3, 26.4, 25.1. Anal. Calcd for C₁₄H₁₈N₂: C, 78.46; H, 8.47; N,
15 13.07. Found: C, 78.15; H, 8.41; N, 13.05
16
17
18
19
20
21
22
23
24
25
26
27
28
29
30
31
32

33 **5-Methyl-3-(piperidin-1-ylmethyl)-1*H*-indole (19)**. Following the general method for the
34 synthesis of **15** and **19** through *N*-oxide intermediates, reaction of *N,N*-dimethyl-1-(5-methyl-1*H*-
35 indol-3-yl)methanamine (**18**) (40 mg, 0.21 mmol) with H₂O₂ (30 %; 60 μL) in absolute ethanol
36 (85 μL), yielded *N,N*-dimethyl-1-(5-methyl-1*H*-indol-3-yl)methanamine oxide **14** that was
37 immediately used with no further purification Reaction of **14** (32 mg, 0.16 mmol) in piperidine
38 (640 μL) yielded **19** (36 mg, >99%). ¹H NMR (300 MHz, CD₃OD) δ 7.40 (m, 1H, H4), 7.24 (d,
39 1H, *J* = 8.3 Hz, H7), 7.17 (s, 1H, H2), 6.95 (dd, 1H, *J* = 1.3, 8.3 Hz, H6), 3.72 (s, 2H, CH₂), 2.54
40 (m, 4H, H2'), 2.43 (s, 3H, CH₃), 1.60 (m, 4H, H3'), 1.51–1.38 (m, 2H, H4'). Its oxalate salt was
41 prepared by dropwise addition of a solution of oxalic acid 1M (1 equiv) in ethyl acetate, under
42 inert gas, to the compound previously dissolved in ethyl acetate dried over MgSO₄. After 2 h
43 stirring, the salt was isolated by centrifugation, the mother liquid decanted, and the traces of
44
45
46
47
48
49
50
51
52
53
54
55
56
57
58
59
60

1
2
3 solvent removed under vacuum. Mp 186–188 °C. ^{13}C NMR (75.4 MHz, DMSO- d_6) δ 163.9,
4
5 134.3, 128.6, 128.1, 127.7, 123.2, 117.9, 111.6, 102.1, 51.1, 50.6, 22.4, 21.3, 21.2. Anal. Calcd
6
7 for $\text{C}_{15}\text{H}_{20}\text{N}_2 \cdot \text{H}_2\text{O} \cdot \text{C}_2\text{H}_2\text{O}_4$: C, 60.70; H, 7.19; N, 8.33. Found: C, 60.73; H, 6.89; N, 8.29
8
9
10

11
12
13
14
15 **General Method for the synthesis of 1 derivatives 16–18 and 20–38.** The method of Miranda
16
17 et al.⁹² was followed with modifications. Under argon atmosphere, dimethylamine (40%_{aq}) or
18
19 piperidine (1–1.5 equiv) and formaldehyde (37%_{aq}, 1–2 equiv) were stirred in glacial acetic acid
20
21 (0.3–5.5 mL/mmol) for 10 min to form the iminium ion, which was then added to a solution of 5-
22
23 bromo-1*H*-indole or compounds **2–12** (1 equiv) in glacial acetic acid (0.1–2 mL/mmol) at 0 °C.
24
25 After 5 min, reaction was allowed to reach room temperature and was stirred for 2–5 h, until the
26
27 reaction was terminated or no evolution was observed by TLC. Then, NaOH_{aq} (30%) was added
28
29 to get a pH 14. The mixture was extracted with neutralized CH_2Cl_2 (3 × 30 mL/mmol) and the
30
31 organic layer dried over anhydrous Na_2SO_4 , filtered and evaporated.
32
33
34
35

36
37 Oily compounds were salinized to hydrochloride or oxalate salts. Hydrochloride salts were
38
39 prepared by dropwise addition of a solution of hydrochloric acid 1M in diethyl ether (1 equiv),
40
41 under inert gas, to the compounds previously dissolved in ether (10 mL). Oxalate salts were
42
43 prepared by dropwise addition of a solution of oxalic acid 1M in ethyl acetate (1 equiv), under
44
45 inert gas, to the compound previously dissolved in ethyl acetate (10 mL). Both types of salts
46
47 were kept under stirring for 2h, isolated by centrifugation and the traces of solvent removed
48
49 under vacuum. Solvents for the salinization solutions were previously dried over MgSO_4 .
50
51
52

53
54
55 **1-(5-Bromo-1*H*-indol-3-yl)-*N,N*-dimethylmethanamine (16)** Following the general method for
56
57 the synthesis of **1** derivatives **16–18** and **20–38**, reaction of 5-bromo-1*H*-indole (200 mg, 1.02
58
59
60

mmol) with dimethylamine (129 μ L, 1.02 mmol) and formaldehyde (76 μ L, 1.02 mmol) in glacial acetic acid (1 mL) yielded **16** as a brown solid that did not required further purification (234 mg, 80%). Mp 134–137 $^{\circ}$ C. 1 H NMR (300 MHz, CDCl_3) δ 8.35 (bs, 1H, NH), 7.84 (d, 1H, J = 1.6 Hz, H4), 7.32–7.23 (dd, 1H, J = 1.8, 8.4 Hz, H6), 7.20 (d, 1H, J = 8.6 Hz, H7), 7.10 (s, 1H, H2), 3.58 (s, 2H, CH_2), 2.28 [s, 6H, $\text{N}(\text{CH}_3)_2$]. 13 C NMR (75.4 MHz, acetone- d_6) δ 136.6, 130.7, 126.5, 124.8, 123.0, 114.0, 113.8, 112.5, 55.7, 45.5 [$\text{N}(\text{CH}_3)_2$]. Anal. Calcd for $\text{C}_{11}\text{H}_{13}\text{BrN}_2$: C, 52.19; H, 5.18; N, 11.07. Found: C, 51.89; H, 5.12; N, 10.64.

5-Bromo-3-(piperidin-1-ylmethyl)-1H-indole (17). Following the general method for the synthesis of **1** derivatives **16–18** and **20–38**, reaction of 5-bromo-1H-indole (200 mg, 1.02 mmol) with piperidine (99 μ L, 1.02 mmol) and formaldehyde (76 μ L, 1.02 mmol) in glacial acetic acid (0.5 mL) yielded **17** as a yellow solid that did not required further purification (238 mg, 80%). Mp 131–134 $^{\circ}$ C. 1 H NMR (300 MHz, acetone- d_6) δ 10.28 (bs, 1H, NH), 7.89 (d, 1H, J = 2.0 Hz, H4), 7.34 (dd, 1H, J = 0.3, 8.6 Hz, H7), 7.25 (d, 1H, J = 2.3 Hz, H2), 7.20 (dd, 1H, J = 2.0, 8.6 Hz, H6), 3.59 (d, 2H, J = 0.7 Hz, C_3CH_2), 2.38 (m, 4H, H2'), 1.56–1.47 (m, 4H, H3'), 1.45–1.36 (m, 2H, H4'). 13 C NMR (75.4 MHz, acetone- d_6): 136.5, 130.7, 126.3, 124.7, 122.9, 113.9, 113.3, 112.4, 55.2, 55.1, 26.9, 25.4. Anal. Calcd for $\text{C}_{14}\text{H}_{17}\text{BrN}_2$: C, 57.35; H, 5.84; N, 9.55. Found: C, 56.94; H, 5.91; N, 9.32.

1-(1-Benzyl-5-bromo-1H-indol-3-yl)-N,N-dimethylmethanamine (20). Following the general method for the synthesis of **1** derivatives **16–18** and **20–38**, reaction of **2** (97 mg, 0.34 mmol) with dimethylamine (43 μ L, 0.34 mmol) and formaldehyde (25 μ L, 0.34 mmol) in glacial acetic acid (2 mL) yielded **20** as a yellow oil that did not required further purification (114 mg, >99%). 1 H NMR (300 MHz, CDCl_3) δ 7.83 (bd, 1H, J = 1.8 Hz, H4), 7.31–7.19 (m, 4H, Ar), 7.11–7.03

1
2
3 (m, 4H, Ar), 5.24 (s, 2H, NCH₂Ph), 3.55 (s, 2H, C3CH₂), 2.26 [s, 6H, N(CH₃)₂]. Its
4
5 hydrochloride salt was prepared as described above. Mp 209–212 °C. ¹³C NMR (75.4 MHz,
6
7 DMSO-*d*₆) δ 137.3, 134.6, 133.5, 129.6, 128.6, 127.6, 127.0, 124.5, 121.6, 112.9, 112.7, 103.0,
8
9 50.5, 49.4, 41.1. Anal. Calcd for C₁₈H₁₉BrN₂·HCl: C, 56.94; H, 5.31; N, 7.38. Found: C, 56.53;
10
11 H, 5.10; N, 7.05.
12
13

14
15
16 **1-Benzyl-5-bromo-3-(piperidin-1-ylmethyl)-1H-indole (21)**. Following the general method for
17
18 the synthesis of **1** derivatives **16–18** and **20–38**, reaction of **2** (138 mg, 0.48 mmol) with
19
20 piperidine (48 μL, 0.48 mmol) and formaldehyde (35 μL, 0.48 mmol) in glacial acetic acid (0.5
21
22 mL) yielded **21** as a yellow oil that did not required further purification (173 mg, 94%). ¹H NMR
23
24 (300 MHz, CDCl₃) δ 7.86 (d, 1H, *J* = 1.7 Hz, H4), 7.33–7.18 (m, 4H, Ar), 7.10–7.03 (m, 4H,
25
26 Ar), 5.23 (s, 2H, NCH₂Ph), 3.61 (s, 2H, C3CH₂), 2.42 (m, 4H, H2'), 1.57 (m, 4H, H3'), 1.41 (m,
27
28 2H, H4'). Its hydrochloride salt was prepared as described above. Mp 199–202 °C. ¹³C NMR
29
30 (75.4 MHz, D₂O + few drops of acetone-*d*₆ for ppm calibration) δ 137.3, 135.2, 133.9, 130.2,
31
32 129.3, 128.4, 127.4, 125.5, 121.4, 113.9, 113.0, 102.0, 52.5, 51.3, 50.4, 23.2, 21.5. Anal. Calcd
33
34 for C₂₁H₂₃BrN₂·2HCl: C, 55.28; H, 5.52; N, 6.14. Found: C, 54.92; H, 5.33; N, 6.17.
35
36
37
38
39
40

41
42 **1-(1-Benzyl-5-methyl-1H-indol-3-yl)-N,N-dimethylmethanamine (22)**. Following the general
43
44 method for the synthesis of **1** derivatives **16–18** and **20–38**, reaction of **3** (126 mg, 0.57 mmol)
45
46 with dimethylamine (72 μL, 0.57 mmol) and formaldehyde (43 μL, 0.57 mmol) in glacial acetic
47
48 acid (0.6 mL) yielded **22** as a yellow oil that did not required further purification (154 mg,
49
50 97%). ¹H NMR (300 MHz, acetone-*d*₆) δ 7.51 (m, 1H, H4), 7.31–7.13 (m, 7H, Ar), 6.94 (dd, 1H,
51
52 *J* = 1.3, 8.3 Hz, H6), 5.34 (s, 2H, NCH₂Ph), 3.56 (s, 2H, C3CH₂), 2.39 (s, 3H, CH₃), 2.21 [s, 6H,
53
54 N(CH₂)₃]. Its oxalate salt was prepared as described above. Mp 166–169 °C. ¹³C NMR (75.4
55
56
57
58
59
60

MHz, D₂O + few drops of acetone-*d*₆ for the ppm calibration) δ 215.8, 137.8, 134.8, 132.6, 130.9, 129.2, 128.4, 128.2, 127.3, 124.6, 118.3, 111.1, 102.1, 52.4, 50.2, 41.8, 20.8. Anal. Calcd for C₁₉H₂₂N₂·C₂H₂O₄: C, 68.46; H, 6.57; N, 7.60. Found: C, 68.18; H, 6.43; N, 7.26.

1-Benzyl-5-methyl-3-(piperidin-1-ylmethyl)-1*H*-indole (23). Following the general method for the synthesis of **1** derivatives **16–18** and **20–38**, reaction of **3** (254 mg, 1.15 mmol) with piperidine (113 μ L, 1.15 mmol) and formaldehyde (86 μ L, 1.15 mmol) in glacial acetic acid (2 mL) yielded **23** as a yellow oil that did not required further purification (355 mg, 97%). ¹H NMR (300 MHz, acetone-*d*₆) δ 7.53 (m, 1H, H4), 7.30–7.14 (m, 7H, Ar), 6.93 (dd, 1H, *J* = 1.2, 8.3 Hz, H6), 5.32 (s, 2H, NCH₂Ph), 3.60 (d, 2H, *J* = 0.7 Hz, C3CH₂), 2.44–2.37 (m, 4H, H2'), 2.40 (s, 3H, CH₃), 1.53 (m, 4H, H3'), 1.42 (m, 2H, H4'). Its oxalate salt was prepared as described above. Mp 172–174 °C. ¹³C NMR (75.4 MHz, DMSO-*d*₆) δ 164.6, 137.8, 134.3, 132.0, 128.7, 128.5, 128.4, 127.4, 127.0, 123.5, 118.4, 110.3, 102.1, 51.0, 50.2, 49.3, 22.4, 21.4, 21.1. Anal. Calcd for C₂₂H₂₆N₂·C₂H₂O₄: C, 70.57; H, 6.91; N, 6.86. Found: C, 70.36; H, 6.86; N, 6.59.

1-(5-Bromo-1-butyl-1*H*-indol-3-yl)-*N,N*-dimethylmethanamine (24). Following the general method for the synthesis of **1** derivatives **16–18** and **20–38**, reaction of **4** (240 mg, 0.95 mmol) with dimethylamine (120 μ L, 0.95 mmol) and formaldehyde (72 μ L, 0.95 mmol) in glacial acetic acid (1 mL) yielded **24**, which was further purified by automatized flash chromatography with ethyl acetate/hexane mixtures as eluent, obtaining a yellow oil (316 mg, >99%). ¹H NMR (300 MHz, CDCl₃) δ 7.80 (d, 1H, *J* = 1.7 Hz, H4), 7.25 (dd, 1H, *J* = 1.9, 8.7 Hz, H6), 7.16 (d, 1H, *J* = 8.7 Hz, H7), 7.02 (s, 1H, H2), 4.05 (t, 2H, *J* = 7.0 Hz, NCH₂(CH₂)₂CH₃), 3.54 (s, 2H, C3CH₂), 2.25 (s, 6H, N(CH₃)₂), 1.78 (m, 2H, NCH₂CH₂CH₂ CH₃), 1.37–1.23 (m, 2H, N(CH₂)₂CH₂CH₃), 0.92 (t, 3H, *J* = 7.3 Hz, CH₃). Its hydrochloride salt was prepared as described above. Mp 84–88

1
2
3 °C. ^{13}C NMR (75.4 MHz, DMSO- d_6) δ 134.6, 133.1, 129.4, 124.3, 121.4, 112.6, 112.4, 102.3,
4
5 50.5, 45.5, 41.0, 31.7, 19.3, 13.5. Anal. Calcd for $\text{C}_{15}\text{H}_{21}\text{BrN}_2\cdot 2\text{HCl}$: C, 47.14; H, 6.07; N, 7.33.
6
7 Found: C, 46.89; H, 6.38; N, 6.95.
8
9

10
11 **5-Bromo-1-butyl-3-(piperidin-1-ylmethyl)-1H-indole (25)**. Following the general method for
12 the synthesis of **1** derivatives **16–18** and **20–38**, reaction of **4** (185 mg, 0.73 mmol) with
13
14 piperidine (73 μL , 0.73 mmol) and formaldehyde (66 μL , 0.88 mmol) in glacial acetic acid (0.5
15
16 mL) yielded **25** as an oil that did not required further purification (279 mg, >99%). ^1H NMR (300
17
18 MHz, CDCl_3) δ 7.83 (d, 1H, $J = 1.8$ Hz, H4), 7.26 (dd, 1H, $J = 1.8, 8.7$ Hz, H6), 7.16 (d, 1H, $J =$
19
20 8.7 Hz, H7), 7.03 (s, 1H, H2), 4.04 (t, 2H, $J = 7.1$ Hz, $\text{NCH}_2(\text{CH}_2)_2\text{CH}_3$), 3.62 (s, 2H, C_3CH_2),
21
22 2.47–2.36 (m, 4H, H2'), 1.79 (m, 2H, $\text{NCH}_2\text{CH}_2\text{CH}_2\text{CH}_3$), 1.58 (m, 4H, H3'), 1.47–1.37 (m, 2H,
23
24 H4'), 1.37–1.24 (m, 2H, $\text{N}(\text{CH}_2)_2\text{CH}_2\text{CH}_3$), 0.93 (t, 3H, $J = 7.3$ Hz, $\text{N}(\text{CH}_2)_3\text{CH}_3$). Its
25
26 hydrochloride salt was prepared as described above. Mp 177–180 °C. ^{13}C NMR (75.4 MHz, D_2O
27
28 + few drops of acetone- d_6 for the ppm calibration) δ 134.8, 133.2, 129.3, 124.8, 120.8, 113.0,
29
30 112.4, 100.8, 52.1, 51.1, 46.0, 31.4, 22.8, 21.1, 19.3, 12.8. Anal. Calcd for $\text{C}_{18}\text{H}_{25}\text{BrN}_2\cdot \text{HCl}$: C,
31
32 56.04; H, 6.79; N, 7.26. Found: C, 55.65; H, 6.63; N, 7.04.
33
34
35
36
37
38
39
40

41 **1-Butyl-5-methyl-3-(piperidin-1-ylmethyl)-1H-indole (26)**. Following the general method for
42 the synthesis of **1** derivatives **16–18** and **20–38**, reaction of **5** (143 mg, 0.76 mmol) with
43
44 piperidine (75 μL , 0.76 mmol) and formaldehyde (57 μL , 0.76 mmol) in glacial acetic acid (0.8
45
46 mL) yielded **26** as an oil that did not required further purification (204 mg, 94%). ^1H NMR (300
47
48 MHz, acetone- d_6) δ 7.50 (m, 1H, H4), 7.25 (d, 1H, $J = 8.3$ Hz, H7), 7.08 (s, 1H, H2), 6.96 (dd,
49
50 1H, $J = 1.4, 8.4$ Hz, H6), 4.10 (t, 2H, $J = 7.0$ Hz, $\text{NCH}_2(\text{CH}_2)_2\text{CH}_3$), 3.58 (d, 2H, $J = 0.5$ Hz,
51
52 C_3CH_2), 2.44–2.36 (m, 7H, H2', CH_3C_5), 1.77 (m, 2H, $\text{NCH}_2\text{CH}_2\text{CH}_2\text{CH}_3$), 1.53 (m, 4H, H3'),
53
54
55
56
57
58
59
60

1
2
3 1.45–1.35 (m, 2H, H4'), 1.35–1.24 [m, 2H, N(CH₂)₂CH₂CH₃], 0.91 (t, 3H, *J* = 7.3 Hz,
4
5 N(CH₂)₃CH₃). Its hydrochloride salt was prepared as described above. Mp 140–143 °C. ¹³C
6
7 NMR (75.4 MHz, D₂O + few drops of acetone-*d*₆ for the ppm calibration) δ 134.7, 132.4, 130.5,
8
9 128.4, 124.1, 118.2, 110.8, 100.8, 52.3, 51.7, 46.2, 31.8, 23.1, 21.4, 20.8, 19.7, 13.2. Anal. Calcd
10
11 for C₁₉H₂₈N₂·HCl: C, 71.11; H, 9.11; N, 8.73. Found: C, 71.20; H, 8.96; N, 8.42.
12
13
14
15

16 **Ethyl 4-(5-bromo-3-((dimethylamino)methyl)-1*H*-indol-1-yl)butanoate (27)**. Following the
17
18 general method for the synthesis of **1** derivatives **16–18** and **20–38**, reaction of **6** (98 mg, 0.32
19
20 mmol) with dimethylamine (60 μL, 0.47 mmol) and formaldehyde (34 μL, 0.47 mmol) in glacial
21
22 acetic acid (1.8 mL) yielded **27** as an oil that did not required further purification (110 mg, 95%).
23
24 ¹H NMR (300 MHz, acetone-*d*₆) δ 7.86 (d, 1H, *J* = 1.9 Hz, H4), 7.38 (d, 1H, *J* = 8.7 Hz, H7),
25
26 7.25 (dd, 1H, *J* = 2.0 Hz, 8.7 Hz, H6), 7.21 (s, 1H, H2), 4.23 [t, 2H, *J* = 7.0 Hz, NCH₂(CH₂)₂],
27
28 4.07 (c, 2H, *J* = 7.1 Hz, COOCH₂CH₃), 3.53 (s, 2H, C3CH₂), 2.28 (t, 2H, *J* = 7.8 Hz,
29
30 CH₂COOCH₂CH₃), 2.18 [s, 6H, N(CH₃)₂], 2.10 (m, 2H, NCH₂CH₂CH₂), 1.19 (t, 3H, *J* = 7.1 Hz,
31
32 COOCH₂CH₃). Its oxalate salt was prepared as described above. Mp 133–135 °C. ¹³C NMR
33
34 (75.4 MHz, CD₃OD) δ 176.3, 165.5, 135.9, 134.0, 130.0, 126.0, 121.7, 114.2, 113.2, 102.6, 62.6,
35
36 52.7, 46.5, 42.4, 32.2, 25.6, 14.0. Anal. Calcd for C₁₇H₂₃BrN₂O₂·H₂O·C₂H₂O₄: C, 48.01; H,
37
38 5.73; N, 5.89. Found: C, 48.05; H, 5.33; N, 5.45.
39
40
41
42
43
44
45

46 **Ethyl 4-(5-bromo-3-(piperidin-1-ylmethyl)-1*H*-indol-1-yl)butanoate (28)**. Following the
47
48 general method for the synthesis of **1** derivatives **16–18** and **20–38**, reaction of **6** (100 mg, 0.32
49
50 mmol) with piperidine (48 μL, 0.48 mmol) and formaldehyde (36 μL, 0.48 mmol) in glacial
51
52 acetic acid (1.1 mL) yielded **28** as an oil that did not required further purification (133 mg,
53
54 >99%). ¹H NMR (300 MHz, acetone-*d*₆) δ 7.90 (d, 1H, *J* = 1.9 Hz, H4), 7.38 (d, 1H, *J* = 8.7 Hz,
55
56
57
58
59
60

1
2
3 H7), 7.25 (dd, 1H, $J = 2.0, 8.7$ Hz, H6), 7.21 (s, 1H, H2), 4.22 [t, 2H, $J = 7.1$ Hz,
4 NCH₂(CH₂)₂CO], 4.07 (c, 2H, $J = 7.1$ Hz, COOCH₂CH₃), 3.58 (s, 2H, C3CH₂), 2.38 (m, 4H,
5 H2'), 2.28 [t, 2H, $J = 7.1$ Hz, N(CH₂)₂CH₂CO], 2.09 (m, 2H, NCH₂CH₂, CH₂CO), 1.57–1.46 (m,
6 4H, H3'), 1.46–1.35 (m, 2H, H4'), 1.19 (t, 3H, $J = 7.1$ Hz, COOCH₂CH₃). Its oxalate salt was
7 prepared as described above. Mp 158–160 °C. ¹³C NMR (75.4 MHz, CD₃OD) δ 220, 176.0,
8 136.0, 133.9, 130.5, 126.1, 121.8, 114.4, 113.2, 102.5, 62.4, 53.1, 52.0, 46.5, 32.2, 25.8, 23.8,
9 22.2, 14.0. Anal. Calcd for C₂₀H₂₇BrN₂O₂·C₂H₂O₄: C, 53.13; H, 5.88; N, 5.63. Found: C, 53.16;
10 H, 5.85; N, 5.50.
11
12
13
14
15
16
17
18
19
20
21
22

23 **1-(5-Bromo-1-(prop-2-yn-1-yl)-1H-indol-3-yl)-N,N-dimethylmethanamine (29)**. Following
24 the general method for the synthesis of **1** derivatives **16–18** and **20–38**, reaction of **7** (126 mg,
25 0.54 mmol) with dimethylamine (68 μL, 0.538 mmol) and formaldehyde (40 μL, 0.54 mmol) in
26 glacial acetic acid (1 mL) yielded **29** as an oil that did not required further purification (154 mg,
27 98%). ¹H NMR (300 MHz, acetone-*d*₆) δ 7.88 (d, 1H, $J = 1.9$ Hz, H4), 7.44 (d, 1H, $J = 8.7$ Hz,
28 H7), 7.29 (m, 2H, H6, H2), 5.04 (d, 2H, $J = 2.5$ Hz, NCH₂CCH), 3.53 (s, 2H, C3CH₂), 2.94 (t,
29 1H, $J = 2.5$ Hz, NCH₂CCH), 2.19 (s, 6H, N(CH₃)₂). Its oxalate salt was prepared as described
30 above. Mp 161–163 °C. ¹³C NMR (75.4 MHz, DMSO-*d*₆) δ 163.7, 134.4, 132.6, 129.7, 124.8,
31 121.7, 113.2, 112.7, 103.5, 78.6, 76.4, 50.5, 41.3, 35.6. Anal. Calcd for
32 C₁₄H₁₅BrN₂·H₂O·2C₂H₂O₄: C, 44.19; H, 4.33; N, 5.73. Found: C, 44.15; H, 4.02; N, 5.78.
33
34
35
36
37
38
39
40
41
42
43
44
45
46
47

48 **5-Bromo-3-(piperidin-1-ylmethyl)-1-(prop-2-yn-1-yl)-1H-indole (30)**. Following the general
49 method for the synthesis of **1** derivatives **16–18** and **20–38**, reaction of **7** (230 mg, 0.98 mmol)
50 with piperidine (97 μL, 0.98 mmol) and formaldehyde (74 μL, 0.98 mmol) in glacial acetic acid
51 (1 mL) yielded **30** as a wax, which did not required further purification (320 mg, 98%). Mp 67–
52
53
54
55
56
57
58
59
60

70 °C. ¹H NMR (300 MHz, acetone-*d*₆) δ 7.91 (d, 1H, *J* = 2.0 Hz, H4), 7.44 (dd, 1H, *J* = 0.4, 8.7 Hz, H7), 7.31–7.27 (m, 2H, H4,H2), 5.04 (d, 2H, *J* = 2.5 Hz, NCH₂CCH), 3.57 (s, 2H, C3CH₂), 2.95 (t, 1H, *J* = 2.5 Hz, NCH₂CCH), 2.38 (m, 4H, H2'), 1.56–1.49 (m, 4H, H3'), 1.44–1.41 (m, 2H, H4'). ¹³C NMR (75.4 MHz, acetone-*d*₆) δ 136.1, 131.4, 129.2, 125.0, 123.3, 113.4, 113.0, 112.4, 79.1, 74.8, 55.1, 54.9, 36.1, 26.9, 25.3. Anal. Calcd for C₁₇H₁₉BrN₂: C, 61.64; H, 5.78; N, 8.46. Found: C, 61.21; H, 5.97; N, 8.60.

***N,N*-Dimethyl-1-(5-methyl-1-(prop-2-yn-1-yl)-1*H*-indol-3-yl)methanamine (31).** Following the general method for the synthesis of **1** derivatives **16–18** and **20–38**, reaction of **8** (236 mg, 1.39 mmol) with dimethylamine (177 μL, 1.39 mmol) and formaldehyde (105 μL, 1.39 mmol) in glacial acetic acid (1.8 mL) yielded **31** as an oil that did not required further purification (282 mg, 90%). ¹H NMR (300 MHz, acetone-*d*₆) δ 7.50 (m, 1H, H4), 7.33 (d, 1H, *J* = 8.3 Hz, H7), 7.17 (s, 1H, H2), 7.02 (dd, 1H, *J* = 1.6, 8.4 Hz, H6), 4.95 (d, 2H, *J* = 2.6 Hz, NCH₂CCH), 3.53 (s, 2H, C3CH₂), 2.90 (t, 1H, *J* = 2.5 Hz, NCH₂CCH), 2.41 (bs, 3H, CH₃C5), 2.19 (s, 6H, N(CH₃)₂). Its oxalate salt was prepared as described above. Mp 136–138 °C. ¹³C NMR (75.4 MHz, D₂O + few drops of acetone-*d*₆ for the ppm calibration) δ 165.0, 134.0, 131.4, 130.9, 128.0, 124.3, 118.0, 110.4, 102.2, 78.3, 74.1, 51.9, 41.5, 35.6, 20.4. Anal. Calcd for C₁₅H₁₈N₂·H₂O·C₂H₂O₄: C, 61.07; H, 6.63; N, 8.38. Found: C, 60.69; H, 6.27; N, 8.75

5-Methyl-3-(piperidin-1-ylmethyl)-1-(prop-2-yn-1-yl)-1*H*-indole (32). Following the general method for the synthesis of **1** derivatives **16–18** and **20–38**, reaction of **8** (190 mg, 1.12 mmol) with piperidine (111 μL, 1.12 mmol) and formaldehyde (84 μL, 1.12 mmol) in glacial acetic acid (0.5 mL) yielded **32** as an oil that did not required further purification (287 mg, 96%). ¹H NMR (300 MHz, CDCl₃) δ 7.48 (m, 1H, H4), 7.27 (d, 1H, *J* = 11.6 Hz, H7), 7.13 (s, 1H, H2), 7.07 (dd,

1
2
3
4
5
6
7
8
9
10
11
12
13
14
15
16
17
18
19
20
21
22
23
24
25
26
27
28
29
30
31
32
33
34
35
36
37
38
39
40
41
42
43
44
45
46
47
48
49
50
51
52
53
54
55
56
57
58
59
60

1H, $J = 2.1, 12.5$ Hz, H6), 4.81 (d, 2H, $J = 3.8$ Hz, NCH₂CCH), 3.68 (s, 2H, C3CH₂), 2.86 (s, 1H, NCH₂CCH), 2.57–2.39 (m, 7H, H2', CH₃C5), 1.68–1.51 (m, 4H, H3'), 1.49–1.38 (m, 2H, H4'). Its oxalate salt was prepared as described above. Mp 115–118 °C. ¹³C NMR (75.4 MHz, DMSO-*d*₆) δ 164.1, 134.0, 131.2, 129.0, 128.4, 123.6, 118.5, 110.2, 102.4, 78.8, 76.0, 51.0, 50.1, 35.4, 22.4, 21.4, 21.2. Anal. Calcd for C₁₈H₂₂N₂·2H₂O·C₂H₂O₄: C, 61.21; H, 7.19; N, 7.14. Found: C, 61.51; H, 6.80; N, 7.02.

5-Bromo-1-(4-chlorobutyl)-3-(piperidin-1-ylmethyl)-1H-indole (33). Following the general method for the synthesis of **1** derivatives **16–18** and **20–38**, reaction of **9** (311 mg, 1.08 mmol) with piperidine (107 μ L, 1.08 mmol) and formaldehyde (81 μ L, 1.08 mmol) in glacial acetic acid (0.9 mL) yielded **33**, which was further purified by trituration with diethyl ether, obtaining a yellow oil (419 mg, >99%). ¹H NMR (300 MHz, acetone-*d*₆) δ 7.89 (dd, 1H, $J = 0.3, 1.9$ Hz, H4), 7.38 (d, 1H, $J = 8.5$ Hz, H7), 7.23 (m, 2H, H6, H2), 4.18 [t, 2H, $J = 6.9$ Hz, NCH₂(CH₂)₃Cl], 3.58 (m, 4H, CH₂Cl, C3CH₂), 2.37 (m, 4H, H2'), 2.02–1.70 (m, 4H, NCH₂CH₂CH₂CH₂Cl), 1.56–1.45 (m, 4H, H3'), 1.45–1.35 (m, 2H, H4'). ¹³C NMR (75.4 MHz, DMSO-*d*₆) δ 146.0, 140.8, 139.3, 134.4, 132.9, 122.3, 122.1, 121.9, 64.8, 64.7, 55.7, 54.9, 40.4, 38.1, 36.6, 35.0. Anal. Calcd for C₁₈H₂₄BrClN₂: C, 56.34; H, 6.30; N, 7.30. Found: C, 56.42; H, 6.46; N, 7.02.

1-(4-Chlorobutyl)-5-methyl-3-(piperidin-1-ylmethyl)-1H-indole (34). Following the general method for the synthesis of **1** derivatives **16–18** and **20–38**, reaction of **10** (155 mg, 0.70 mmol) with piperidine (69 μ L, 0.70 mmol) and formaldehyde (52 μ L, 0.70 mmol) in glacial acetic acid (1.5 mL) yielded **34** as a yellow oil that did not required further purification (229 mg, >99%). ¹H NMR (300 MHz, acetone-*d*₆) δ 7.50 (m, 1H, H4), 7.27 (d, 1H, $J = 8.4$ Hz, H7), 7.09 (s, 1H, H2),

6.97 (dd, 1H, $J = 1.4, 8.4$ Hz, H6), 4.16 [t, 2H, $J = 6.8$ Hz, $\text{NCH}_2(\text{CH}_2)_3\text{Cl}$], 3.60–3.53 (m, 4H, CH_2Cl , C_3CH_2), 2.44–2.33 (m, 4H, H2'), 2.40 (s, 3H, CH_3C_5), 1.93 [m, 2H, $\text{NCH}_2\text{CH}_2(\text{CH}_2)_2\text{Cl}$], 1.72 [m, 2H, $\text{N}(\text{CH}_2)_2\text{CH}_2\text{CH}_2\text{Cl}$], 1.56–1.47 (m, 4H, H3'), 1.45–1.36 (m, 2H, H4'). Its oxalate salt was prepared as described above. Mp 130–133 °C. ^{13}C NMR (75.4 MHz, $\text{DMSO}-d_6$) δ 164.2, 134.2, 131.3, 128.5, 128.2, 123.4, 121.4, 118.5, 110.1, 51.3, 46.8, 44.9, 44.9, 29.4, 27.2, 24.7, 22.7, 21.2. Anal. Calcd for $\text{C}_{19}\text{H}_{27}\text{ClN}_2 \cdot \text{C}_2\text{H}_2\text{O}_4$: C, 61.68; H, 7.15; N, 6.85. Found: C, 61.31; H, 7.05; N, 6.65.

1-(5-Bromo-1-(4-(piperidin-1-yl)butyl)-1H-indol-3-yl)-N,N-dimethylmethanamine (35).

Following the general method for the synthesis of **1** derivatives **16–18** and **20–38**, reaction of **11** (92 mg, 0.27 mmol) with dimethylamine (35 μL , 0.27 mmol) and formaldehyde (21 μL , 0.27 mmol) in glacial acetic acid (1.8 mL) yielded **35** as an oil that did not required further purification (115 mg, >99%). ^1H NMR (300 MHz, $\text{acetone}-d_6$) δ 7.85 (d, 1H, $J = 2.0$ Hz, H4), 7.39 (d, 1H, $J = 8.7$ Hz, H7), 7.23 (m, 2H, H6, H2), 4.18 [t, 2H, $J = 7.1$ Hz, $\text{NCH}_2(\text{CH}_2)_3\text{N}$], 3.52 (s, 2H, C_3CH_2), 2.30–2.19 [m, 6H, $\text{N}(\text{CH}_2)_3\text{CH}_2\text{N}$, H2'], 2.17 [s, 6H, $\text{N}(\text{CH}_3)_2$], 1.83 [m, 2H, $\text{NCH}_2\text{CH}_2(\text{CH}_2)_2\text{N}$], 1.53–1.32 [m, 8H, $\text{N}(\text{CH}_2)_2\text{CH}_2\text{CH}_2\text{N}$, H3', H4']. Its oxalate salt was prepared as described above. Mp 123–125 °C. ^{13}C NMR (75.4 MHz, D_2O + few drops of $\text{acetone}-d_6$ for ppm calibration) δ 165.7, 135.2, 133.2, 129.4, 125.5, 121.2, 113.6, 112.6, 102.1, 56.5, 53.3, 52.1, 45.9, 41.8, 26.8, 23.0, 21.4, 21.2. Anal. Calcd for $\text{C}_{20}\text{H}_{30}\text{BrN}_3 \cdot \text{H}_2\text{O} \cdot 2\text{C}_2\text{H}_2\text{O}_4$: C, 48.82; H, 6.15; N, 7.12. Found: C, 49.26; H, 6.04; N, 6.75.

5-Bromo-1-(4-(piperidin-1-yl)butyl)-3-(piperidin-1-ylmethyl)-1H-indole (36). Following the

general method for the synthesis of **1** derivatives, reaction of **11** (70 mg, 0.21 mmol) with piperidine (21 μL , 0.21 mmol) and formaldehyde (16 μL , 0.21 mmol) in glacial acetic acid (400

1
2
3
4
5
6
7
8
9
10
11
12
13
14
15
16
17
18
19
20
21
22
23
24
25
26
27
28
29
30
31
32
33
34
35
36
37
38
39
40
41
42
43
44
45
46
47
48
49
50
51
52
53
54
55
56
57
58
59
60

μL) yielded **36** as an oil that did not required further purification (90 mg, >99%). ^1H NMR (300 MHz, acetone- d_6) δ 7.99 (d, 1H, J = 1.8 Hz, H4), 7.37 (d, 1H, J = 8.7 Hz, H7), 7.22 (dd, 1H, J_{4-6} = 1.8, 8.7 Hz, H6), 7.19 (s, 1H, H2), 4.16 [t, 2H, J = 7.1 Hz, $\text{NCH}_2(\text{CH}_2)_3\text{N}$], 3.56 (s, 2H, C_3CH_2), 2.37 (m, 4H, H_2''), 2.29–2.18 [m, 6H, $\text{N}(\text{CH}_2)_3\text{CH}_2\text{N}$, H_2'], 1.83 [m, 2H, $\text{NCH}_2\text{CH}_2(\text{CH}_2)_2\text{N}$], 1.55–1.34 [m, 14H, $\text{N}(\text{CH}_2)_2\text{CH}_2\text{CH}_2\text{N}$, H_3' , H_4' , H_3'' , H_4'']. Its oxalate salt was prepared as described above. Mp 90–92 °C. ^{13}C NMR (75.4 MHz, D_2O + few drops of acetone- d_6 for the ppm calibration) δ 168.2, 135.1, 133.3, 129.8, 125.4, 121.4, 113.7, 112.6, 101.8, 56.5, 53.3, 52.5, 51.4, 45.9, 26.8, 23.2, 23.0, 21.5, 21.2. Anal. Calcd for $\text{C}_{23}\text{H}_{34}\text{BrN}_3 \cdot 2\text{C}_2\text{H}_2\text{O}_4$: C, 52.94; H, 6.25; N, 6.86. Found: C, 52.89; H, 6.67; N, 6.86.

***N,N*-Dimethyl-1-(5-methyl-1-(4-(piperidin-1-yl)butyl)-1*H*-indol-3-yl)methanamine (37).**

Following the general method for the synthesis of **1** derivatives, reaction of **12** (93 mg, 0.34 mmol) with dimethylamine (44 μL , 0.34 mmol) and formaldehyde (26 μL , 0.34 mmol) in glacial acetic acid (0.6 mL) yielded **37** as a yellow oil that did not required further purification (102 mg, 91%). ^1H NMR (300 MHz, acetone- d_6) δ 7.46 (m, 1H, H4), 7.28 (d, 1H, J = 8.3 Hz, H7), 7.11 (s, 1H, H2), 6.96 (dd, 1H, J = 1.5, 8.3 Hz, H6), 4.13 [t, 2H, J = 7.0 Hz, $\text{NCH}_2(\text{CH}_2)_3\text{N}$], 3.53 (s, 2H, C_3CH_2), 2.40 (s, 3H, CH_3C_5), 2.31–2.20 [m, 6H, $\text{N}(\text{CH}_2)_3\text{CH}_2\text{N}$, H_2'], 2.18 [s, 6H, $\text{N}(\text{CH}_3)_2$], 1.82 [m, 2H, $\text{NCH}_2\text{CH}_2(\text{CH}_2)_2\text{N}$], 1.54–1.44 (m, 4H, H_3'), 1.44–1.34 (m, 2H, H_4'). Its oxalate salt was prepared as described above. Mp 146–149 °C. ^{13}C NMR (75.4 MHz, $\text{DMSO-}d_6$) δ 164.6, 134.1, 131.6, 128.6, 128.1, 123.4, 118.4, 110.1, 102.3, 55.3, 52.0, 50.9, 45.1, 41.2, 26.7, 22.4, 21.4, 21.2, 20.7. Anal. Calcd for $\text{C}_{21}\text{H}_{35}\text{N}_3 \cdot \text{H}_2\text{O} \cdot 2\text{C}_2\text{H}_2\text{O}_4$: C, 57.13; H, 7.48; N, 7.99. Found: C, 57.49; H, 7.11; N, 7.61.

1
2
3 **5-Methyl-1-(4-(piperidin-1-yl)butyl)-3-(piperidin-1-ylmethyl)-1*H*-indole (38)**. Following the
4
5 general method for the synthesis of **1** derivatives, reaction of **12** (120 mg, 0.44 mmol) with
6
7 piperidine (44 μ L, 0.44 mmol) and formaldehyde (33 μ L, 0.444 mmol) in glacial acetic acid (1.8
8
9 mL) yielded **38** as an oil that did not required further purification (162 mg, 96%). ^1H NMR (300
10
11 MHz, acetone- d_6) δ 7.48 (m, 1H, H4), 7.27 (m, 1H, H7), 7.07 (s, 1H, H2), 6.95 (dd, 1H, J = 2.1,
12
13 12.3 Hz, H6), 4.11 [t, 2H, J = 10.4 Hz, $\text{NCH}_2(\text{CH}_2)_3\text{N}$], 3.56 (d, 2H, J = 1.0 Hz, C_3CH_2), 2.44-
14
15 2.32 (m, 7H, H2'', CH_3C_5), 2.30–2.16 [m, 6H, $\text{N}(\text{CH}_2)_3\text{CH}_2\text{N}$, H2'], 1.80 [m, 2H,
16
17 $\text{NCH}_2\text{CH}_2(\text{CH}_2)_2\text{N}$], 1.59–1.33 [m, 14H, $\text{N}(\text{CH}_2)_2\text{CH}_2\text{CH}_2\text{N}$, H3', H4', H3'', H4'']. Its oxalate
18
19 salt was prepared as described above. Mp 64–66 $^\circ\text{C}$. ^{13}C NMR (75.4 MHz, DMSO - d_6) δ 164.2,
20
21 134.0, 131.7, 128.6, 128.4, 123.4, 118.4, 110.1, 101.7, 55.4, 52.1, 51.3, 50.5, 45.1, 26.6, 22.5,
22
23 22.5, 21.4, 21.4, 21.2, 20.8.. Anal. Calcd for $\text{C}_{24}\text{H}_{37}\text{N}_3 \cdot \text{H}_2\text{O} \cdot 2\text{C}_2\text{H}_2\text{O}_4$: C, 59.45; H, 7.66; N, 7.43.
24
25 Found: C, 59.82; H, 7.36; N, 7.18.
26
27
28
29
30
31
32

33 **Molecular Modeling.** The structure and conformational analysis of ligand **23** were obtained
34
35 with the Monte Carlo method in Spartan10. The most stable conformer were subsequently
36
37 optimized with ab initio Hartree-Fock 6-31G* calculations, and selected for docking studies. The
38
39 3D structure of the Protein Phosphatase 2A bound to OA was obtained from the Protein Data
40
41 Bank (PDB ID: 2IE4).⁷⁰ All solvent molecules and the co-crystallized ligand okadaic acid were
42
43 removed from the complex. Molecular docking calculations for PP2A and compound **23** were
44
45 undertaken using Molegro Virtual Docker 3.0,⁹³ under a large enough sphere able to
46
47 accommodate the cavity, centering it on the binding site of the protein structure, to allow the
48
49 ligand to search the best pose. Different orientations of the ligands were searched and ranked
50
51 based on their energy scores. Poses with the best both energies and conformations were selected
52
53
54
55
56
57
58
59
60

1
2
3 for further 3D analysis. MolDock Score was used as algorithm, which is adapted from the
4
5 Differential Evolution (DE) algorithm.
6
7
8
9

10
11 **Pharmacology. Data Analysis.** Data are shown as means \pm standard error of the mean (SEM).
12
13 Statistical significant differences ($p \leq 0.05$) were calculated by ANOVA followed by a Newman-
14
15 Keuls or Dunnett's post hoc test, obtained using the Prism software 5.0 (GraphPad) for a Mac
16
17 OS X-operated computer.
18
19

20
21 **Experimental Use of Animals.** All efforts were made to minimize the number of animals used
22
23 for the experiments and their suffering. We followed the guidelines of the EU Council Directive.
24
25 Experiments were approved by the Ethics Committee of the Universidad Autónoma de Madrid,
26
27 Spain.
28
29

30
31 **Culture and treatment of neuroblastoma cells.** SH-SY5Y cells were maintained similarly to
32
33 what was previously described.⁶³ For neuroprotection assays, cells were subcultured in 48 well
34
35 plates at a seeding density of 7×10^4 cells per well. Before cells achieved confluence,
36
37 compounds dissolved in media supplemented with 10% fetal bovine serum (FBS) were
38
39 preincubated for 24 h. For coincubation, media was replaced by fresh new media with 1% FBS,
40
41 compounds and the corresponding toxic stimulus. When coincubation finished, cell viability or
42
43 phosphatase activities were measured.
44
45
46
47
48

49
50 **Culture and treatment of rat hippocampal slices.** Hippocampal slices from 2-month-old
51
52 Sprague-Dawley rats were extracted, isolated, and treated with glutamate according to
53
54 experimental procedures previously described.⁵¹ After stabilization at 34 °C for 45 min,
55
56
57
58
59
60

1
2
3 compounds and glutamate dissolved in medium were coincubated for 4 h and cell viability was
4
5 measured by the method of the MTT reduction.
6
7

8
9 **Culture and treatment of rat motor cortical neurons.** Embryos from 18 to 19 days of
10 pregnancy were obtained by caesarean operation. After decapitation of the embryos and
11 dissection of the brains, meninges were removed and the motor cortex was isolated. The
12 fragments obtained from several embryos were subjected to mechanic digestion. Motor cortical
13 neurons were resuspended in Neurobasal medium with 2% B-27 and seeded in poly-*D*-lysine-
14 pre-coated 48-well plates (density of 3×10^4 cells per well). Neuronal cultures were allowed to
15 grow 8 to 10 days until a dense neuronal network was observed. Tested compounds dissolved in
16 medium were preincubated for 24 h, after which veratridine was directly added into the wells and
17 allowed to coincubate for another 24 h. The cell viability was assessed by the method of the
18 MTT reduction.
19
20
21
22
23
24
25
26
27
28
29
30
31

32
33 **Measurement of cell viability in SH-SY5Y cells, hippocampal slices and motor cortex**
34 **neurons.** Cell viability was assessed by the quantitative colorimetric method of the MTT
35 reduction.⁷⁶ Briefly, only in living cells the MTT (3-[4,5-dimethylthiazol-2-yl]-2,5-
36 diphenyltetrazolium bromide, yellow-colored) is chemically reduced by mitochondrial
37 dehydrogenase enzymes, thus being cell viability indirectly measured as mitochondrial activity
38 of healthy cells. The reduced MTT is a purple-colored formazan derivative, which is dissolved in
39 DMSO and offers a concentration-dependent colorimetric signal at 540 nm. MTT dissolved in
40 water at 10 mg/mL was added to the wells (final concentration of 0.3 mg/mL) and was incubated
41 in the dark at 37 °C for 2 h (SH-SY5Y cells) or 30 min (hippocampal slices and neurons). After
42 harvesting the medium, cells and tissue were lysed and the formazan dissolved with 300 μ L, 200
43 μ L or 120 μ L of DMSO, as if it is SH-SY5Y cells, hippocampal slices or neurons, respectively.
44
45
46
47
48
49
50
51
52
53
54
55
56
57
58
59
60

1
2
3 Absorbance was measured at 540 nm in a colorimetric plate reader (FLUOstar Optima, BMG,
4 Germany). Data were expressed as percentage of cell viability, taking as 100% the obtained
5 absorbance value in untreated cells.
6
7
8
9

10
11 **Measurement of phosphatase activity in SH-SY5Y cells.** The Biosciences Phosphatase Assay
12 Kit (Cat. #786-453) was used to measure the activity of phosphatases. Briefly, *p*-nitrophenyl
13 phosphate (pNPP) acts as chromogenic substrate for the phosphatases, generating *p*-nitrophenol
14 when dephosphorylated, which is deprotonated under alkaline conditions to produce *p*-
15 nitrophenolate that has a strong absorption at 405 nm. For total phosphatase activity, cellular
16 media was removed and 50 μ L of assay buffer and substrate (10 mM) were added to each well.
17
18 The reaction mixture was incubated in the dark at 37 °C for 30 min and the absorbance was
19 measured at 405 nm (FLUOstar Optima, BMG, Germany). Ser/Thr phosphatase activity was
20 measured by adding NaVO₃ 1 mM to the buffer. Data were reported as percentage of
21 phosphatase activity, taking as 100% the obtained absorbance value in untreated cells.
22
23
24
25
26
27
28
29
30
31
32
33
34
35

36 **Measurement of cytosolic Ca²⁺ in SH-SY5Y cells.** Free cytosolic Ca²⁺ concentration was
37 measured using the fluorescent Ca²⁺ indicator Fluo-4/AM (Fluo-4 acetoxymethylester). SH-
38 SY5Y cells were seeded onto 96-well black plates at a density of 10⁵ cells per well, achieving
39 confluence after 48 h. Cells were washed with Krebs-Hepes solution (KH, in mM: 144 NaCl, 5.9
40 KCl, 1.2 MgCl₂, 2 CaCl₂, 11 D-glucose, 10 HEPES, pH 7.4). Cells were loaded with 10 μ M
41 Fluo-4/AM and 0.2% pluronic acid in KH and incubated for 45 min at 37 °C in the dark. Then,
42 cells were washed twice with KH to remove the excess of probe. Tested compounds were
43 incubated 10 min before KCl 70 mM was applied to evoke the increment of cytosolic Ca²⁺. To
44 normalize Fluo-4 signals, Triton X-100 (5%) and 1 M MnCl₂ were applied to register both
45
46
47
48
49
50
51
52
53
54
55
56
57
58
59
60

1
2
3 maximal and minimal fluorescence, respectively. The experiments were analyzed at excitation
4 and emission wavelengths of 485 and 520 nm, respectively, and fluorescence was measured in a
5
6 fluorescence microplate reader (FLUOstar Optima, BMG, Germany). Data were calculated as a
7
8 percentage of $F_{\max} - F_{\min}$.
9
10

11
12
13 **Culture and measurement of Ca^{2+} currents in chromaffin cells.** Bovine chromaffin cells were
14
15 isolated and cultured according to a protocol previously described.⁹⁴ All experiments were
16
17 performed at room temperature (24 ± 2 °C) on cells from 1 to 4 days after culture. I_{Ca} were
18
19 measured under the whole cell configuration of the patch-clamp technique.⁹⁵ During recording,
20
21 cells were constantly perfused with a standard control solution at pH 7.4 containing (mM): 145
22
23 NaCl, 5.6 KCl, 1.2 MgCl_2 , 2 CaCl_2 , 11 glucose and 10 HEPES/NaOH. Cells were internally
24
25 dialysed with an intracellular solution containing (in mM): 100 Cs-glutamate, 14 EGTA, 20
26
27 tetraethylammonium, 10 NaCl, 5 ATP-Mg, 0.3 GTP-Na, and 20 HEPES/CsOH (pH 7.3). Whole-
28
29 cell recordings were made with fire-polished borosilicate pipettes (resistance 2-5 $\text{M}\Omega$) that were
30
31 mounted on the headstage of an EPC-9 patch-clamp amplifier (HEKA Elektronik, Lambrecht,
32
33 Germany), allowing cancellation of capacitative transients and compensation of series resistance.
34
35 Data were recorded in a frequency of 20 kHz by using PULSE v8.74 software (HEKA
36
37 Elektronik). Data analyses were performed with PULSE v8.74 program (HEKA Elektronik).
38
39 Coverslips containing the cells were placed on a chamber installed on the stage of a inverted
40
41 microscope. The external solutions were exchanged using miniature solenoid valves coupled to a
42
43 multi-barrel concentration clamp apparatus, placing the common outlet within the 100 μm of the
44
45 cell to be patched. The flow rate was 1 mL/min and was regulated by gravity. Nifedipine and
46
47 different compounds were perfused as indicated. In order to measure I_{Ca} , cells were held at -80
48
49
50
51
52
53
54
55
56
57
58
59
60

1
2
3 mV and, each 20-s, single depolarizing pulses were applied to voltages where I_{Ca} peak was
4
5 reached.
6
7

8 9 10 ANCILLARY INFORMATION

11 12 13 **Supporting Information**

14
15
16 1H NMR spectra of compounds **2–38** and ^{13}C NMR spectra of tested compounds **15–38**,
17
18 scheme of patch-clamp experimental protocols, in vitro toxicity experiments with the tested
19
20 compounds. This material is available free of charge via the Internet at <http://pubs.acs.org>.
21
22
23

24 25 26 **Corresponding Authors**

27
28
29 *For C.d.l.R.: phone, +34-914972765; fax, +34-914973453; E-mail,
30
31 cristobal.delosrios@inv.uam.es
32
33

34 35 36 **Present Addresses**

37
38
39
40 ||Instituto de Investigación Sanitaria, Fundación Jiménez Díaz, Universidad Autónoma de
41
42 Madrid, Avda. Reyes Católicos, 2, 28040 Madrid, Spain.
43
44
45

46 47 48 **ACKNOWLEDGMENTS**

49
50
51
52
53 This work was supported by grants from Instituto de Salud Carlos III, Ministerio de Sanidad,
54
55 Spain (Proyectos de Investigación en Salud: PI13/00789 to CdIR) and Ministerio de Economía y
56
57 Competitividad, Spain (SAF 2013-44108-P to L.G.). R.L.C is granted by Universidad Autónoma
58
59
60

1
2
3 de Madrid, Spain. We thank the continued support of Fundación de Investigación Biomédica,
4
5 Hospital Universitario de la Princesa, and Fundación Teófilo Hernando.
6
7
8
9
10

11 12 ABBREVIATIONS USED 13

14
15 A β , amyloid β peptide ; AD, Alzheimer's disease; ChE, cholinesterases; I_{Ca}, Ca²⁺ currents;
16 I/V, current vs. voltage; MTT, 3-(4,5-dimethylthiazol-2-yl)-2,5-diphenyltetrazolium bromide;
17
18 NFT, neurofibrillary tangles; NMDA, *N*-methyl-*D*-aspartate; OA, okadaic acid; *p*NPP, *p*-
19 nitrophenylphosphate; PP1, phosphoprotein phosphatase 1; PP2A, phosphoprotein phosphatase
20
21 2A; PPP, phosphoprotein phosphatases; TTX, tetrodotoxin; VGCC, voltage-gated Ca²⁺ channels;
22
23 VGNC, voltage-gated Na⁺ channels; ω -ctx, ω -conotoxin.
24
25
26
27
28
29
30
31
32

33 34 35 36 37 38 39 40 41 42 43 44 45 46 47 48 49 50 51 52 53 54 55 56 57 58 59 60

References

- (1) Alzheimer, A. Über einen eigenartige erkrankung der hirnrinde. *Alleomag. Z. Psych.* **1907**, *64*, 146–148.
- (2) Scheltens, P.; Blennow, K.; Breteler, M. M.; de Strooper, B.; Frisoni, G. B.; Salloway, S.; Van der Flier, W. M. Alzheimer's disease. *Lancet* **2016**, DOI: 10.1016/S0140-6736(15)01124-1
- (3) Anand, R.; Gill, K. D.; Mahdi, A. A. Therapeutics of Alzheimer's disease: Past, present and future. *Neuropharmacology* **2014**, *76 Pt A*, 27–50.
- (4) Mullard, A. Sting of Alzheimer's failures offset by upcoming prevention trials. *Nat. Rev. Drug Discovery* **2012**, *11*, 657–660.

1
2
3 (5) Herrup, K. The case for rejecting the amyloid cascade hypothesis. *Nat. Neurosci.* **2015**, *18*,
4 794–799.
5

6
7
8 (6) Iqbal, K.; Liu, F.; Gong, C. X. Tau and neurodegenerative disease: the story so far. *Nat. Rev.*
9 *Neurol.* **2016**, *12*, 15–27.
10

11
12 (7) Salahuddin, P.; Fatima, M. T.; Abdelhameed, A. S.; Nusrat, S.; Khan, R. H. Structure of
13 amyloid oligomers and their mechanisms of toxicities: Targeting amyloid oligomers using novel
14 therapeutic approaches. *Eur. J. Med. Chem.* **2016**, *114*, 41–58.
15
16

17
18 (8) Bulic, B.; Pickhardt, M.; Mandelkow, E. M.; Mandelkow, E. Tau protein and tau
19 aggregation inhibitors. *Neuropharmacology* **2010**, *59*, 276–289.
20
21

22
23 (9) Gong, C. X.; Iqbal, K. Hyperphosphorylation of microtubule-associated protein tau: a
24 promising therapeutic target for Alzheimer disease. *Curr. Med. Chem.* **2008**, *15*, 2321–2328.
25
26

27
28 (10) Carreiras, M. C.; Mendes, E.; Perry, M. J.; Francisco, A. P.; Marco-Contelles, J. The
29 multifactorial nature of Alzheimer's disease for developing potential therapeutics. *Curr. Top.*
30 *Med. Chem.* **2013**, *13*, 1745–1770.
31
32

33
34 (11) Guzior, N.; Wieckowska, A.; Panek, D.; Malawska, B. Recent development of
35 multifunctional agents as potential drug candidates for the treatment of Alzheimer's disease.
36
37
38
39
40
41
42 *Curr. Med. Chem.* **2015**, *22*, 373–404.

43
44 (12) Fang, L.; Appenroth, D.; Decker, M.; Kiehnopf, M.; Lupp, A.; Peng, S.; Fleck, C.; Zhang,
45 Y.; Lehmann, J. NO-donating tacrine hybrid compounds improve scopolamine-induced
46 cognition impairment and show less hepatotoxicity. *J. Med. Chem.* **2008**, *51*, 7666–7669.
47
48

49
50 (13) Simoni, E.; Serafini, M. M.; Bartolini, M.; Caporaso, R.; Pinto, A.; Necchi, D.; Fiori, J.;
51 Andrisano, V.; Minarini, A.; Lanni, C.; Rosini, M. Nature-inspired multifunctional ligands:
52
53
54
55
56
57
58
59
60

1
2
3 focusing on amyloid-based molecular mechanisms of Alzheimer's disease. *ChemMedChem* **2016**,

4
5 DOI: 10.1002/cmdc.201500422.

6
7
8 (14) Di Martino, R. M.; De Simone, A.; Andrisano, V.; Bisignano, P.; Bisi, A.; Gobbi, S.;
9
10 Rampa, A.; Fato, R.; Bergamini, C.; Perez, D. I.; Martinez, A.; Bottegoni, G.; Cavalli, A.;
11
12 Belluti, F. Versatility of the curcumin scaffold: discovery of potent and balanced dual BACE-1
13
14 and GSK-3beta inhibitors. *J. Med. Chem.* **2016**, *59*, 531–544.

15
16
17 (15) Bolea, I.; Juarez-Jimenez, J.; de Los Rios, C.; Chioua, M.; Pouplana, R.; Luque, F. J.;
18
19 Unzeta, M.; Marco-Contelles, J.; Samadi, A. Synthesis, biological evaluation, and molecular
20
21 modeling of donepezil and N-[(5-(benzyloxy)-1-methyl-1H-indol-2-yl)methyl]-N-methylprop-2-
22
23 yn-1-amine hybrids as new multipotent cholinesterase/monoamine oxidase inhibitors for the
24
25 treatment of Alzheimer's disease. *J. Med. Chem.* **2011**, *54*, 8251–8270.

26
27
28 (16) Romero, A.; Egea, J.; Gonzalez-Munoz, G. C.; Martin de Saavedra, M. D.; del Barrio, L.;
29
30 Rodriguez-Franco, M. I.; Conde, S.; Lopez, M. G.; Villarroja, M.; de los Rios, C.
31
32 ITH12410/SC058: a new neuroprotective compound with potential in the treatment of
33
34 Alzheimer's disease. *ACS Chem. Neurosci.* **2014**, *5*, 770–775.

35
36
37 (17) Martinez-Sanz, F. J.; Lajarin-Cuesta, R.; Moreno-Ortega, A. J.; Gonzalez-Lafuente, L.;
38
39 Fernandez-Morales, J. C.; Lopez-Arribas, R.; Cano-Abad, M. F.; de los Rios, C. Benzothiazepine
40
41 CGP37157 analogues exert cytoprotection in various in vitro models of neurodegeneration. *ACS*
42
43 *Chem. Neurosci.* **2015**, *6*, 1626–1636.

44
45
46 (18) Egea, J.; de los Rios, C. 1,8-Naphthyridine derivatives as cholinesterases inhibitors and cell
47
48 Ca²⁺ regulators, a multitarget strategy for Alzheimer's disease. *Curr. Top. Med. Chem.* **2011**, *11*,
49
50 2807–2823.
51
52
53
54
55
56
57
58
59
60

1
2
3 (19) Samadi, A.; Valderas, C.; de los Rios, C.; Bastida, A.; Chioua, M.; Gonzalez-Lafuente, L.;
4 Colmena, I.; Gandia, L.; Romero, A.; Del Barrio, L.; Martin-de-Saavedra, M. D.; Lopez, M. G.;
5 Villarroya, M.; Marco-Contelles, J. Cholinergic and neuroprotective drugs for the treatment of
6 Alzheimer and neuronal vascular diseases. II. Synthesis, biological assessment, and molecular
7 modelling of new tacrine analogues from highly substituted 2-aminopyridine-3-carbonitriles.

8
9
10
11
12
13
14
15 *Bioorg. Med. Chem.* **2011**, *19*, 122–133.

16
17 (20) Zundorf, G.; Reiser, G. Calcium dysregulation and homeostasis of neural calcium in the
18 molecular mechanisms of neurodegenerative diseases provide multiple targets for
19 neuroprotection. *Antioxid. Redox Signaling* **2011**, *14*, 1275–1288.

20
21
22 (21) Riascos, D.; Nicholas, A.; Samaeekia, R.; Yukhananov, R.; Mesulam, M. M.; Bigio, E. H.;
23 Weintraub, S.; Guo, L.; Geula, C. Alterations of Ca(2+)-responsive proteins within cholinergic
24 neurons in aging and Alzheimer's disease. *Neurobiol. Aging* **2014**, *35*, 1325–1333.

25
26 (22) Resende, R.; Pereira, C.; Agostinho, P.; Vieira, A. P.; Malva, J. O.; Oliveira, C. R.
27 Susceptibility of hippocampal neurons to Abeta peptide toxicity is associated with perturbation
28 of Ca²⁺ homeostasis. *Brain Res.* **2007**, *1143*, 11–21.

29
30 (23) Mark, R. J.; Hensley, K.; Butterfield, D. A.; Mattson, M. P. Amyloid beta-peptide impairs
31 ion-motive ATPase activities: evidence for a role in loss of neuronal Ca²⁺ homeostasis and cell
32 death. *J. Neurosci.* **1995**, *15*, 6239–6249.

33
34 (24) Fernandez-Morales, J. C.; Arranz-Tagarro, J. A.; Calvo-Gallardo, E.; Maroto, M.; Padin, J.
35 F.; Garcia, A. G. Stabilizers of neuronal and mitochondrial calcium cycling as a strategy for
36 developing a medicine for Alzheimer's disease. *ACS Chem. Neurosci.* **2012**, *3*, 873–883.

37
38 (25) Nimmrich, V.; Eckert, A. Calcium channel blockers and dementia. *Br. J. Pharmacol.* **2013**,
39
40
41
42
43
44
45
46
47
48
49
50
51
52
53
54
55
56
57
58
59
60
169, 1203–1210.

- 1
2
3 (26) Zamponi, G. W. Targeting voltage-gated calcium channels in neurological and psychiatric
4 diseases. *Nat. Rev. Drug Discovery* **2016**, *15*, 19–34.
5
6
7
8 (27) Asakura, K.; Matsuo, Y.; Kanemasa, T.; Ninomiya, M. P/Q-type Ca²⁺ channel blocker
9 omega-agatoxin IVA protects against brain injury after focal ischemia in rats. *Brain Res.* **1997**,
10 776, 140–145.
11
12
13 (28) Berman, R. F.; Verweij, B. H.; Muizelaar, J. P. Neurobehavioral protection by the neuronal
14 calcium channel blocker ziconotide in a model of traumatic diffuse brain injury in rats. *J.*
15 *Neurosurg.* **2000**, *93*, 821–828.
16
17
18 (29) Hosaka, T.; Yamamoto, Y. L.; Diksic, M. Efficacy of retrograde perfusion of the cerebral
19 vein with verapamil after focal ischemia in rat brain. *Stroke* **1991**, *22*, 1562–1566.
20
21
22 (30) Paris, D.; Bachmeier, C.; Patel, N.; Quadros, A.; Volmar, C. H.; Laporte, V.; Ganey, J.;
23 Beaulieu-Abdelahad, D.; Ait-Ghezala, G.; Crawford, F.; Mullan, M. J. Selective antihypertensive
24 dihydropyridines lower Abeta accumulation by targeting both the production and the clearance
25 of Abeta across the blood-brain barrier. *Mol. Med.* **2011**, *17*, 149–162.
26
27
28 (31) Lopez-Arrieta, J. M.; Birks, J. Nimodipine for primary degenerative, mixed and vascular
29 dementia. *Cochrane Database Syst. Rev.* **2002**, CD000147.
30
31
32 (32) Lajarin-Cuesta, R.; Arribas, R. L.; De Los Rios, C. Ligands for Ser/Thr phosphoprotein
33 phosphatases: a patent review (2005-2015). *Expert Opin. Ther. Pat.* **2016**, *26*, 389–407.
34
35
36 (33) Tell, V.; Hilgeroth, A. Recent developments of protein kinase inhibitors as potential AD
37 therapeutics. *Front. Cell. Neurosci.* **2013**, *7*, 189.
38
39
40 (34) Lovestone, S.; Boada, M.; Dubois, B.; Hull, M.; Rinne, J. O.; Huppertz, H. J.; Calero, M.;
41 Andres, M. V.; Gomez-Carrillo, B.; Leon, T.; del Ser, T. A phase II trial of tideglusib in
42 Alzheimer's disease. *J. Alzheimer's Dis.* **2015**, *45*, 75–88.
43
44
45
46
47
48
49
50
51
52
53
54
55
56
57
58
59
60

- 1
2
3 (35) Zhang, M.; Yogesha, S. D.; Mayfield, J. E.; Gill, G. N.; Zhang, Y. Viewing
4 serine/threonine protein phosphatases through the eyes of drug designers. *FEBS J.* **2013**, *280*,
5 4739–4760.
6
7
8
9
10 (36) Liu, F.; Grundke-Iqbal, I.; Iqbal, K.; Gong, C. X. Contributions of protein phosphatases
11 PP1, PP2A, PP2B and PP5 to the regulation of tau phosphorylation. *Eur. J. Neurosci.* **2005**, *22*,
12 1942–1950.
13
14
15
16
17 (37) Gong, C. X.; Liu, F.; Wu, G.; Rossie, S.; Wegiel, J.; Li, L.; Grundke-Iqbal, I.; Iqbal, K.
18 Dephosphorylation of microtubule-associated protein tau by protein phosphatase 5. *J.*
19 *Neurochem.* **2004**, *88*, 298–310.
20
21
22
23
24 (38) Vogelsberg-Ragaglia, V.; Schuck, T.; Trojanowski, J. Q.; Lee, V. M. PP2A mRNA
25 expression is quantitatively decreased in Alzheimer's disease hippocampus. *Exp. Neurol.* **2001**,
26 *168*, 402–412.
27
28
29
30
31 (39) Sontag, E.; Luangpirom, A.; Hladik, C.; Mudrak, I.; Ogris, E.; Speciale, S.; White, C. L.,
32 3rd. Altered expression levels of the protein phosphatase 2A ABalphaC enzyme are associated
33 with Alzheimer disease pathology. *J. Neuropathol. Exp. Neurol.* **2004**, *63*, 287–301.
34
35
36
37 (40) Tanimukai, H.; Grundke-Iqbal, I.; Iqbal, K. Up-regulation of inhibitors of protein
38 phosphatase-2A in Alzheimer's disease. *Am. J. Pathol.* **2005**, *166*, 1761–1771.
39
40
41
42 (41) Chen, S.; Li, B.; Grundke-Iqbal, I.; Iqbal, K. I1PP2A affects tau phosphorylation via
43 association with the catalytic subunit of protein phosphatase 2A. *J. Biol. Chem.* **2008**, *283*,
44 10513–10521.
45
46
47
48
49 (42) Longin, S.; Zwaenepoel, K.; Louis, J. V.; Dilworth, S.; Goris, J.; Janssens, V. Selection of
50 protein phosphatase 2A regulatory subunits is mediated by the C terminus of the catalytic
51 Subunit. *J. Biol. Chem.* **2007**, *282*, 26971–26980.
52
53
54
55
56
57
58
59
60

1
2
3 (43) Sontag, E.; Hladik, C.; Montgomery, L.; Luangpirom, A.; Mudrak, I.; Ogris, E.; White, C.
4
5 L., 3rd. Downregulation of protein phosphatase 2A carboxyl methylation and methyltransferase
6
7 may contribute to Alzheimer disease pathogenesis. *J. Neuropathol. Exp. Neurol.* **2004**, *63*, 1080–
8
9 1091.

10
11
12 (44) Drewes, G.; Mandelkow, E. M.; Baumann, K.; Goris, J.; Merlevede, W.; Mandelkow, E.
13
14 Dephosphorylation of tau protein and Alzheimer paired helical filaments by calcineurin and
15
16 phosphatase-2A. *FEBS Lett.* **1993**, *336*, 425–432.

17
18
19 (45) Sontag, E.; Nunbhakdi-Craig, V.; Lee, G.; Brandt, R.; Kamibayashi, C.; Kuret, J.; White,
20
21 C. L., 3rd; Mumby, M. C.; Bloom, G. S. Molecular interactions among protein phosphatase 2A,
22
23 tau, and microtubules. Implications for the regulation of tau phosphorylation and the
24
25 development of tauopathies. *J. Biol. Chem.* **1999**, *274*, 25490–25498.

26
27
28 (46) Gong, C. X.; Grundke-Iqbal, I.; Iqbal, K. Dephosphorylation of Alzheimer's disease
29
30 abnormally phosphorylated tau by protein phosphatase-2A. *Neuroscience* **1994**, *61*, 765-772.

31
32
33 (47) Ma, O. K.; Sucher, N. J. Molecular interaction of NMDA receptor subunit NR3A with
34
35 protein phosphatase 2A. *Neuroreport* **2004**, *15*, 1447–1450.

36
37
38 (48) Zhu, M.; Wang, J.; Liu, M.; Du, D.; Xia, C.; Shen, L.; Zhu, D. Upregulation of protein
39
40 phosphatase 2A and NR3A-pleiotropic effect of simvastatin on ischemic stroke rats. *PLoS One*
41
42
43 **2012**, *7*, e51552.

44
45
46 (49) Martin, L.; Latypova, X.; Wilson, C. M.; Magnaudeix, A.; Perrin, M. L.; Yardin, C.; Terro,
47
48 F. Tau protein kinases: involvement in Alzheimer's disease. *Ageing Res. Rev.* **2013**, *12*, 289–309.

49
50
51 (50) de Los Rios, C.; Egea, J.; Marco-Contelles, J.; Leon, R.; Samadi, A.; Iriepa, I.; Moraleda,
52
53 I.; Galvez, E.; Garcia, A. G.; Lopez, M. G.; Villarroya, M.; Romero, A. Synthesis, inhibitory
54
55

1
2
3 activity of cholinesterases, and neuroprotective profile of novel 1,8-naphthyridine derivatives. *J.*
4
5 *Med. Chem.* **2010**, *53*, 5129–5143.

6
7
8 (51) Lorrio, S.; Romero, A.; Gonzalez-Lafuente, L.; Lajarin-Cuesta, R.; Martinez-Sanz, F. J.;
9
10 Estrada, M.; Samadi, A.; Marco-Contelles, J.; Rodriguez-Franco, M. I.; Villarroya, M.; Lopez,
11
12 M. G.; de los Rios, C. PP2A ligand ITH12246 protects against memory impairment and focal
13
14 cerebral ischemia in mice. *ACS Chem. Neurosci.* **2013**, *4*, 1267–1277.

15
16
17 (52) Settimo, A. D.; Primofiore, G.; Ferrarini, P. L. Bromoderivatives of gramines. Preparation
18
19 and pharmacological properties. *Eur. J. Med. Chem.* **1983**, *18*, 261–267.

20
21
22 (53) Iwata, S.; Saito, S.; Kon-ya, K.; Shizuri, Y.; Ohizumi, Y. Novel marine-derived halogen-
23
24 containing gamine analogues induce vasorelaxation in isolated rat aorta. *Eur. J. Pharmacol.*
25
26 **2001**, *432*, 63–70.

27
28
29 (54) Pelech, S.; Cohen, P. The protein phosphatases involved in cellular regulation. 1.
30
31 Modulation of protein phosphatases-1 and 2A by histone H1, protamine, polylysine and heparin.
32
33 *Eur. J. Biochem.* **1985**, *148*, 245–251.

34
35
36 (55) Voronkov, M.; Braithwaite, S. P.; Stock, J. B. Phosphoprotein phosphatase 2A: a novel
37
38 druggable target for Alzheimer's disease. *Future Med. Chem.* **2011**, *3*, 821–833.

39
40
41 (56) Lambrecht, C.; Haesen, D.; Sents, W.; Ivanova, E.; Janssens, V. Structure, regulation, and
42
43 pharmacological modulation of PP2A phosphatases. *Methods Mol. Biol.* **2013**, *1053*, 283–305.

44
45
46 (57) Gurer-Orhan, H.; Suzen, S. Melatonin, its metabolites and its synthetic analogs as multi-
47
48 faceted compounds: antioxidant, prooxidant and inhibitor of bioactivation reactions. *Curr. Med.*
49
50 *Chem.* **2015**, *22*, 490–499.

51
52
53 (58) Aiello, F.; Valacchi, G. Synthesis and evaluation of indole based molecules for treatment
54
55 of oxidative stress related diseases. *Curr. Top. Med. Chem.* **2014**, *14*, 2576–2589.

- 1
2
3 (59) Camacho, M. E.; Carrion, M. D.; Lopez-Cara, L. C.; Entrena, A.; Gallo, M. A.; Espinosa,
4 A.; Escames, G.; Acuna-Castroviejo, D. Melatonin synthetic analogs as nitric oxide synthase
5 inhibitors. *Mini Rev. Med. Chem.* **2012**, *12*, 600–617.
6
7
8
9
10 (60) Semenov, B. B.; Granik, V. G. Chemistry of N-(1H-indol-3-ylmethyl)-N,N-dimethylamine
11 (Gramine): A Review. *Pharm. Chem. J.* **2004**, *38*, 287–310.
12
13
14 (61) Palmieri, A.; Petrini, M.; Shaikh, R. R. Synthesis of 3-substituted indoles via reactive
15 alkylideneindolenine intermediates. *Org. Biomol. Chem.* **2010**, *8*, 1259–1270.
16
17
18 (62) Ilic, N.; Habus, I.; Barkawi, L. S.; Park, S.; Stefanic, Z.; Kojic-Prodic, B.; Cohen, J. D.;
19 Magnus, V. Aminoethyl-substituted indole-3-acetic acids for the preparation of tagged and
20 carrier-linked auxin. *Bioorg. Med. Chem.* **2005**, *13*, 3229–3240.
21
22
23 (63) Gonzalez-Lafuente, L.; Egea, J.; Leon, R.; Martinez-Sanz, F. J.; Monjas, L.; Perez, C.;
24 Merino, C.; Garcia-De Diego, A. M.; Rodriguez-Franco, M. I.; Garcia, A. G.; Villarroya, M.;
25 Lopez, M. G.; de Los Rios, C. Benzothiazepine CGP37157 and its isosteric 2'-methyl analogue
26 provide neuroprotection and block cell calcium entry. *ACS Chem. Neurosci.* **2012**, *3*, 519–529.
27
28
29 (64) Sousa, S. R.; Vetter, I.; Ragnarsson, L.; Lewis, R. J. Expression and pharmacology of
30 endogenous Cav channels in SH-SY5Y human neuroblastoma cells. *PLoS One* **2013**, *8*, e59293.
31
32 (65) Vaughan, P. F.; Peers, C.; Walker, J. H. The use of the human neuroblastoma SH-SY5Y to
33 study the effect of second messengers on noradrenaline release. *Gen. Pharmacol.* **1995**, *26*,
34 1191–1201.
35
36
37 (66) Reeve, H. L.; Vaughan, P. F.; Peers, C. Calcium channel currents in undifferentiated
38 human neuroblastoma (SH-SY5Y) cells: actions and possible interactions of dihydropyridines
39 and omega-conotoxin. *Eur. J. Neurosci.* **1994**, *6*, 943–952.
40
41
42
43
44
45
46
47
48
49
50
51
52
53
54
55
56
57
58
59
60

1
2
3 (67) Albillos, A.; Garcia, A. G.; Olivera, B.; Gandia, L. Re-evaluation of the P/Q Ca²⁺ channel
4 components of Ba²⁺ currents in bovine chromaffin cells superfused with solutions containing
5
6 low and high Ba²⁺ concentrations. *Pfluegers Arch.* **1996**, *432*, 1030–1038.
7
8

9
10 (68) Arranz-Tagarro, J. A.; de los Rios, C.; Garcia, A. G.; Padin, J. F. Recent patents on
11 calcium channel blockers: emphasis on CNS diseases. *Expert Opin. Ther. Pat.* **2014**, *24*, 959–
12
13 977.
14
15

16
17 (69) Hillyard, D. R.; Monje, V. D.; Mintz, I. M.; Bean, B. P.; Nadasdi, L.; Ramachandran, J.;
18 Miljanich, G.; Azimi-Zoonooz, A.; McIntosh, J. M.; Cruz, L. J.; Imperial, J. S.; Olivera, B. M. A
19 new Conus peptide ligand for mammalian presynaptic Ca²⁺ channels. *Neuron* **1992**, *9*, 69–77.
20
21
22

23 (70) Xing, Y.; Xu, Y.; Chen, Y.; Jeffrey, P. D.; Chao, Y.; Lin, Z.; Li, Z.; Strack, S.; Stock, J. B.;
24 Shi, Y. Structure of protein phosphatase 2A core enzyme bound to tumor-inducing toxins. *Cell*
25
26
27 **2006**, *127*, 341–353.
28
29

30
31 (71) Sun, L.; Liu, S. Y.; Zhou, X. W.; Wang, X. C.; Liu, R.; Wang, Q.; Wang, J. Z. Inhibition of
32 protein phosphatase 2A- and protein phosphatase 1-induced tau hyperphosphorylation and
33
34 impairment of spatial memory retention in rats. *Neuroscience* **2003**, *118*, 1175–1182.
35
36
37

38 (72) Perez, M.; Hernandez, F.; Gomez-Ramos, A.; Smith, M.; Perry, G.; Avila, J. Formation of
39 aberrant phosphotau fibrillar polymers in neural cultured cells. *Eur. J. Biochem.* **2002**, *269*,
40
41 1484–1489.
42
43

44 (73) Swingle, M.; Ni, L.; Honkanen, R. E. Small-molecule inhibitors of ser/thr protein
45
46 phosphatases: specificity, use and common forms of abuse. *Methods Mol. Biol.* **2007**, *365*, 23–38.
47
48

49 (74) McAvoy, T.; Nairn, A. C. Serine/threonine protein phosphatase assays. *Curr. Protoc. Mol.*
50
51 *Biol.* **2010**, *Chapter 18*, Unit18 18.
52
53
54
55
56
57
58
59
60

- 1
2
3 (75) Denu, J. M.; Lohse, D. L.; Vijayalakshmi, J.; Saper, M. A.; Dixon, J. E. Visualization of
4 intermediate and transition-state structures in protein-tyrosine phosphatase catalysis. *Proc. Natl.*
5
6 *Acad. Sci. U S A* **1996**, *93*, 2493–2498.
7
8
9
10 (76) Denizot, F.; Lang, R. Rapid colorimetric assay for cell growth and survival. Modifications
11 to the tetrazolium dye procedure giving improved sensitivity and reliability. *J. Immunol.*
12
13 *Methods* **1986**, *89*, 271–277.
14
15
16
17 (77) Nicolau, S. M.; de Diego, A. M.; Cortes, L.; Egea, J.; Gonzalez, J. C.; Mosquera, M.;
18 Lopez, M. G.; Hernandez-Guijo, J. M.; Garcia, A. G. Mitochondrial Na⁺/Ca²⁺-exchanger
19 blocker CGP37157 protects against chromaffin cell death elicited by veratridine. *J. Pharmacol.*
20 *Exp. Ther.* **2009**, *330*, 844–854.
21
22
23
24 (78) Kolok, S.; Nagy, J.; Szombathelyi, Z.; Tarnawa, I. Functional characterization of sodium
25 channel blockers by membrane potential measurements in cerebellar neurons: prediction of
26 compound preference for the open/inactivated state. *Neurochem. Int.* **2006**, *49*, 593–604.
27
28
29
30 (79) Koh, P. O. Melatonin attenuates decrease of protein phosphatase 2A subunit B in ischemic
31 brain injury. *J. Pineal Res.* **2012**, *52*, 57–61.
32
33
34 (80) Martinez-Sanz, F. J.; Lajarin-Cuesta, R.; Gonzalez-Lafuente, L.; Moreno-Ortega, A. J.;
35 Punzon, E.; Cano-Abad, M. F.; de Los Rios, C. Neuroprotective profile of pyridothiazepines
36 with blocking activity of the mitochondrial Na⁽⁺⁾/Ca⁽²⁺⁾ exchanger. *Eur. J. Med. Chem.* **2016**,
37 *109*, 114–123.
38
39
40 (81) Lewerenz, J.; Maher, P. Chronic Glutamate Toxicity in Neurodegenerative Diseases-What
41 is the Evidence? *Front. Neurosci.* **2015**, *9*, 469.
42
43
44 (82) Chan, S. F.; Sucher, N. J. An NMDA receptor signaling complex with protein phosphatase
45 2A. *J. Neurosci.* **2001**, *21*, 7985–7992.
46
47
48
49
50
51
52
53
54
55
56
57
58
59
60

- 1
2
3 (83) Zimmer, E. R.; Leuzy, A.; Souza, D. O.; Portela, L. V. Inhibition of protein phosphatase
4
5 2A: focus on the glutamatergic system. *Mol. Neurobiol.* **2015**, DOI: 10.1007/s12035-015-9321-0
6
7
8 (84) Triggler, D. J. Drug targets in the voltage-gated calcium channel family: why some are and
9
10 some are not. *Assay Drug Dev. Technol.* **2003**, *1*, 719–733.
11
12 (85) Baell, J. B.; Holloway, G. A. New substructure filters for removal of pan assay interference
13
14 compounds (PAINS) from screening libraries and for their exclusion in bioassays. *J. Med. Chem.*
15
16 **2010**, *53*, 2719–2740.
17
18 (86) Na, Y. M.; Le Borgne, M.; Pagniez, F.; Le Baut, G.; Le Pape, P. Synthesis and antifungal
19
20 activity of new 1-halogenobenzyl-3-imidazolylmethylindole derivatives. *Eur. J. Med. Chem.*
21
22 **2003**, *38*, 75–87.
23
24 (87) Evans, D. A.; Scheidt, K. A.; Fandrick, K. R.; Lam, H. W.; Wu, J. Enantioselective indole
25
26 Friedel–Crafts alkylations catalyzed by bis(oxazoliny)pyridine-scandium(III) triflate
27
28 complexes. *J. Am. Chem. Soc.* **2003**, *125*, 10780–10781.
29
30 (88) Evans, D. A.; Fandrick, K. R.; Song, H. J. Enantioselective Friedel–Crafts alkylations of
31
32 alpha,beta-unsaturated 2-acyl imidazoles catalyzed by bis(oxazoliny)pyridine-scandium(III)
33
34 triflate complexes. *J. Am. Chem. Soc.* **2005**, *127*, 8942–8943.
35
36 (89) Haider, N.; Kabicher, T.; Kaferbock, J.; Plenk, A. Synthesis and in-vitro antitumor activity
37
38 of 1-[3-(indol-1-yl)prop-1-yn-1-yl]phthalazines and related compounds. *Molecules* **2007**, *12*,
39
40 1900–1909.
41
42 (90) Martelli, C.; Coronello, M.; Dei, S.; Manetti, D.; Orlandi, F.; Scapecchi, S.; Novella
43
44 Romanelli, M.; Salerno, M.; Mini, E.; Teodori, E. Structure-activity relationships studies in a
45
46 series of N,N-bis(alkanol)amine aryl esters as P-glycoprotein (Pgp) dependent multidrug
47
48 resistance (MDR) inhibitors. *J. Med. Chem.* **2010**, *53*, 1755–1762.
49
50
51
52
53
54
55
56
57
58
59
60

1
2
3 (91) Henry, D. W.; Leete, E. Amine oxides. I. Gramine oxide. *J. Am. Chem. Soc.* **1957**, *79*,
4
5 5254–5256.
6

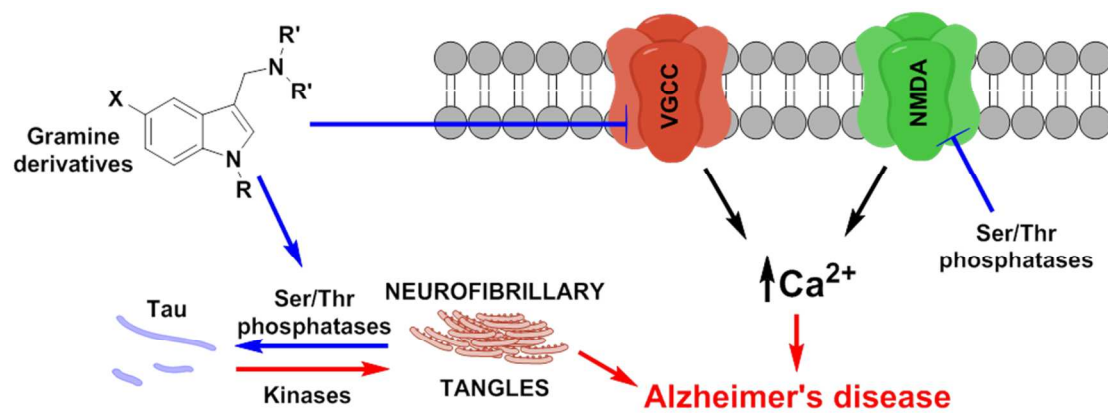
7
8 (92) Miranda, S.; Lopez-Alvarado, P.; Avendano, C.; Menendez, J. C. Convenient synthesis of
9
10 highly functionalized, 3,4-disubstituted indole building blocks. *Open Org. Chem. J.* **2007**, *1*, 1–
11
12 12.
13

14
15 (93) Thomsen, R.; Christensen, M. H. MolDock: a new technique for high-accuracy molecular
16
17 docking. *J. Med. Chem.* **2006**, *49*, 3315–3321.
18

19
20 (94) Moro, M. A.; Lopez, M. G.; Gandia, L.; Michelena, P.; Garcia, A. G. Separation and
21
22 culture of living adrenaline- and noradrenaline-containing cells from bovine adrenal medullae.
23
24 *Anal. Biochem.* **1990**, *185*, 243–248.
25

26
27 (95) Hamill, O. P.; Marty, A.; Neher, E.; Sakmann, B.; Sigworth, F. J. Improved patch-clamp
28
29 techniques for high-resolution current recording from cells and cell-free membrane patches.
30
31 *Pfluegers Arch.* **1981**, *391*, 85–100.
32
33
34
35
36
37
38
39
40
41
42
43
44
45
46
47
48
49
50
51
52
53
54
55
56
57
58
59
60

Table of Contents graphic



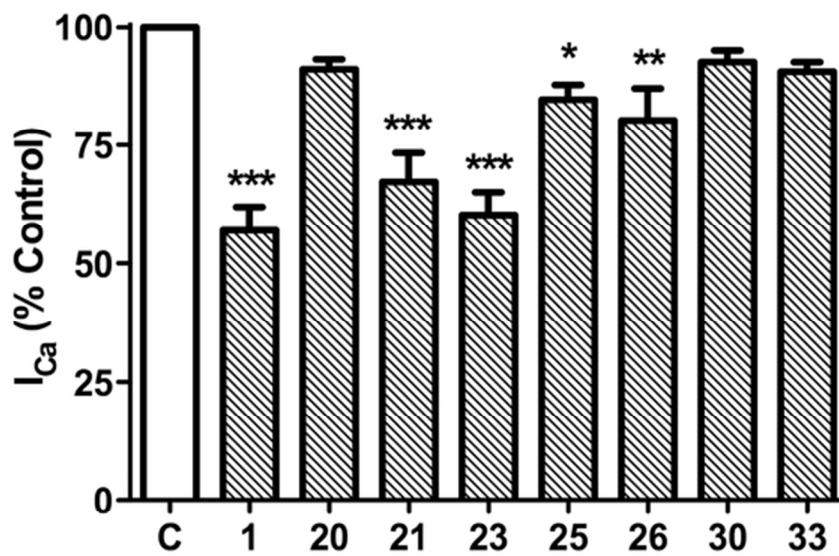


Figure 2
56x37mm (300 x 300 DPI)

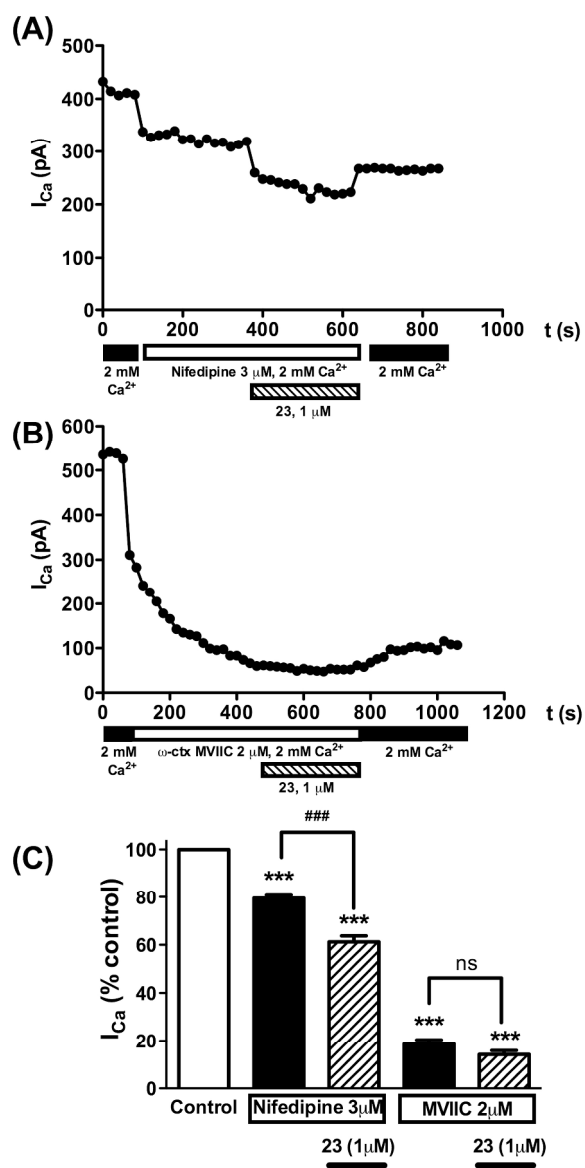


Figure 3
161x308mm (300 x 300 DPI)

1
2
3
4
5
6
7
8
9
10
11
12
13
14
15
16
17
18
19
20
21
22
23
24
25
26
27
28
29
30
31
32
33
34
35
36
37
38
39
40
41
42
43
44
45
46
47
48
49
50
51
52
53
54
55
56
57
58
59
60

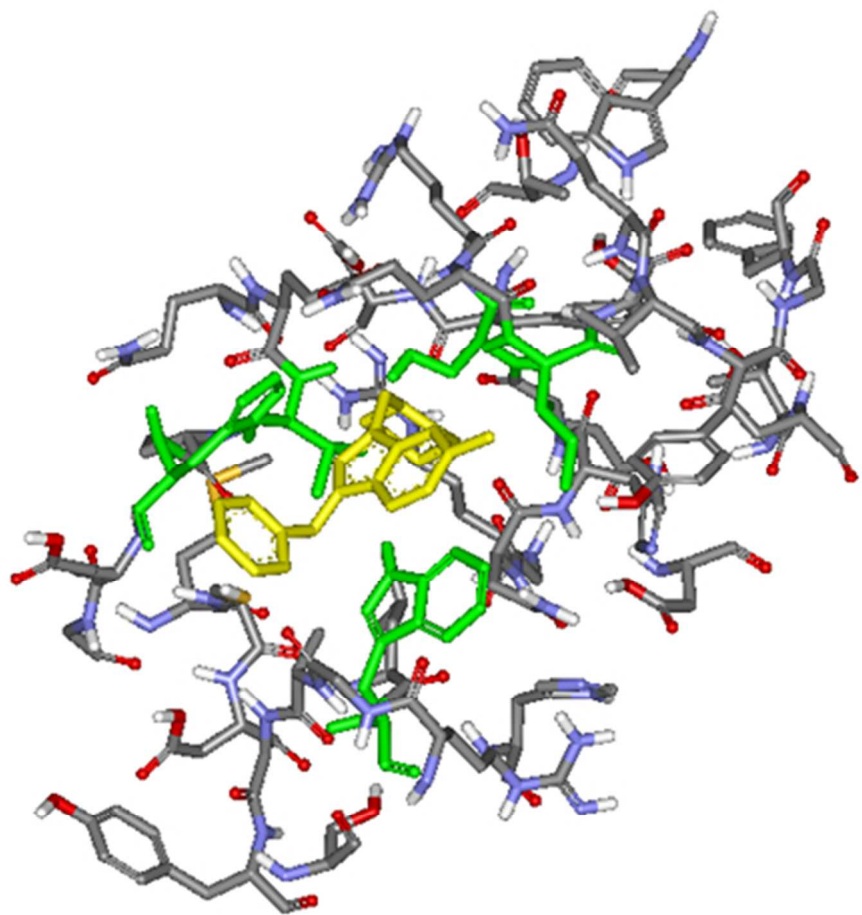


Figure 4A
77x79mm (150 x 150 DPI)

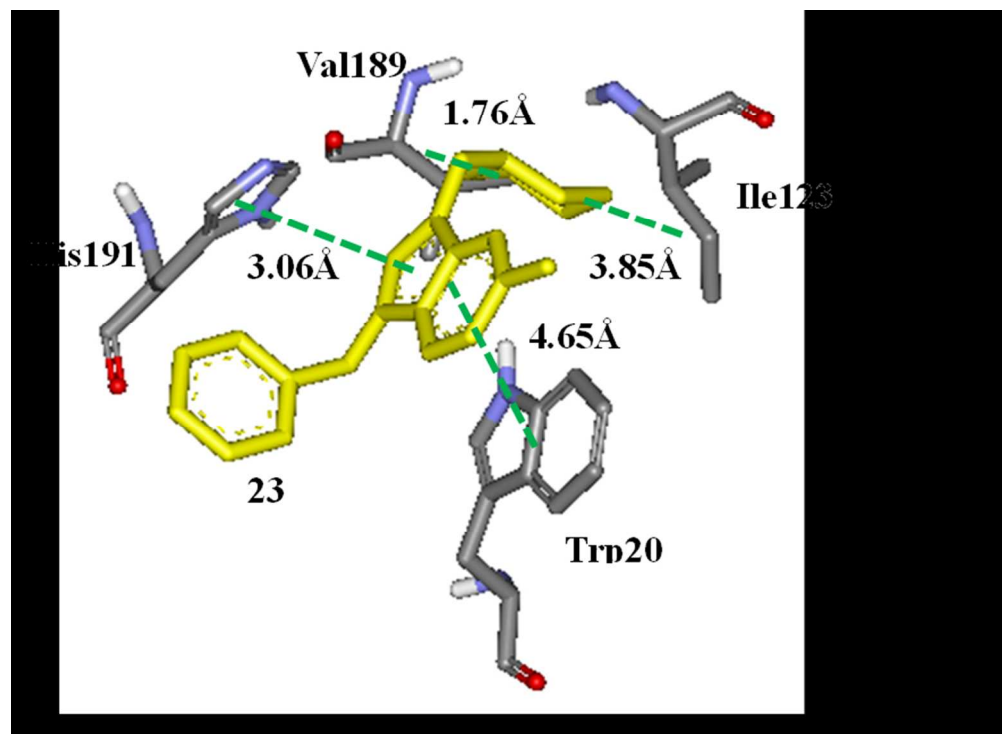


Figure 4B
149x109mm (150 x 150 DPI)

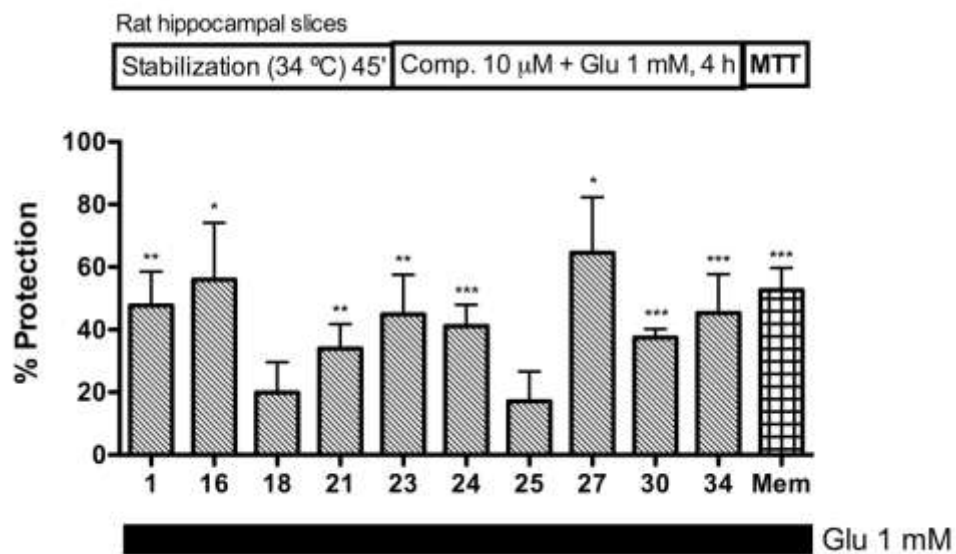


Figure 5
101x60mm (300 x 300 DPI)